Manifold Learning under Noise: Classical Multidimensional Scaling and Random Forests

by

Gongkai Li

A dissertation submitted to The Johns Hopkins University in conformity with the requirements for the degree of Doctor of Philosophy.

Baltimore, Maryland

May, 2019

Abstract

Classical multidimensional scaling (CMDS) is a widely used method in dimensionality reduction and manifold learning. The method takes in a dissimilarity matrix and outputs a low-dimensional configuration matrix based on a spectral decomposition. In this dissertation, we present three noise models and analyze the resulting configuration matrices, or embeddings. In particular, we show that under each of the three noise models the resulting embedding gives rise to a central limit theorem. We also provide compelling simulations and real data illustrations of these central limit theorems. This perturbation analysis represents a significant advancement over previous results regarding classical multidimensional scaling behavior under randomness.

Now the second part is for Random Forest CMDS is a special case of a more general procedure called Manifold Learning, which is essentially required to achieve quality inferences for modern high-dimensional datasets. Many manifold learning methods have been proposed, each with their own advantages and disadvantages. In this dissertation, building off recent advances in supervised learning, we modify the leading supervised decision forest method to support unsupervised learning, and therefore

ABSTRACT

also nonlinear manifold learning. The key differentiator between our Unsupervised Randomer Forest (URerf) and other manifold learning techniques is that URerF operates on low-dimensional sparse linear combinations of features, rather than either the full observed dimensionality, or one-dimensional marginals. We quantify the efficacy of URerF by computing precision-recall curves relative to the true latent manifold or class label (when it is known). Empirical results on simulated data demonstrate that URerF is robust to high-dimensional noise, where as other methods, such as Isomap and UMAP, quickly deteriorate in such settings.

Primary Reader: Carey E. Priebe

Secondary Reader: Minh Tang

Acknowledgments

The past five years in graduate school has been nothing but pure joy and excitement for me. Much of the previous statement is only true because my advisor, Carey Priebe, without whom this journey will be impossible, let along enjoyable, so I want to thank him for his support and valuable advice at all levels. To Minh Tang and Avanti Athreya, I want to express my uttermost admiration for putting up with me and explain things to me when I am confused (which is most of the time). I also want to thank my co-authors and collaborators, including Nicolas Charon, Vince Lyzinski, Youngser Park, Joshua Vogelstein and Randal Burns, who have all offered their help with patience in discussions over the past few years.

Special thanks to Dan Naiman, Daniel Robinson for their time and suggestions in my Candidacy Exam and Raman Arora and Katia Consani for their time and suggestions in my Graduate Board Exam.

I also want express my appreciation for the faculty and staff of the Applied Mathematicss and Statistics Department at Johns Hopkins University. In particular, my thanks to John Wierman, Edward Scheinerman, Fred Torcaso, Donniell Fishkind,

ACKNOWLEDGMENTS

Tamás Budavári for their kindness advice; and to Kristin Bechtel, Sandy Kirt, and Ann Gibbins for their help. My deepest thanks to my friends: Joshua Cape, Heather Pastolic, Wei-Chun Hung, Hsi-Wei Hsieh, Jordan Yoder, Theo Drivas, Chu-Chi Lee, Meghana Madhyastha and Hayden Helm for keeping me sane during the past couple years. Finally, my warmest thanks to my parents, Weiyang Li and Huiping Xu, whose unconditional love made me who I am (well, at least the good part), and also to my first wife Cindy, for putting up with me.

Dedication

This thesis is dedicated to my parents and the Schaufelds

Contents

List of Tables

List of Figures

Chapter 1

Introduction

1.1 Multidimensional Scaling

Inference based on dissimilarities is of fundamental importance in statistics, data mining and machine learning Pekalska and Duin [2005], with applications ranging from neuroscience Vogelstein et al. [2014] to psychology Carroll and Chang [1970] to economics Machado and Mata [2015]. In each of these fields, rather than directly observing the feature values of the objects, often we observe only the dissimilarities or "distances" between pairs of objects (inter-point distances). A common approach to dimensionality reduction and subsequent inference problems involving dissimilarities is to embed the observed distances into some (usually Euclidean) space to recover a configuration that faithfully preserves observed distances, and then proceed to perform inference based on the resulting configuration Borg and Groenen [2005], Cox and

Cox [2008], de Leeuw and Heiser [1982], Torgerson [1952]. The popular classical multidimensional scaling (CMDS) dimensionality reduction method provides an example of such an embedding scheme into Euclidean space, in which we have readily available tools to perform statistical inference. Furthermore, CMDS also forms the basis for several other more recent approaches to nonlinear dimension reduction and manifold learning Chen and Buja [2009], Schölkopf et al. [1998], such as Isomap Tenenbaum et al. [2000a] and Random Forest manifold learning Criminisi and Shotton [2013] among others.

Although widely used, the behavior of CMDS under randomness remains largely unexplored. Several recent papers have highlighted this omission. Zhang et al. [2016] write "Despite the popularity of multi-dimensional scaling, very little is known about to what extent the distances between the embedded points could faithfully reflect the true pairwise distances when observed with noise."; Fan et al. [2018] write "[W]e are not aware of any statistical results measuring the performance of MDS under randomness, such as perturbation analysis when the objects are sampled from a probabilistic model." and Peterfreund and Gavish [2018] write "To the best of our knowledge, the literature does not offer a systematic treatment on the influence of ambient noise on MDS embedding quality." This paper addresses this acknowledged gap in the literature.

1.2 Randomer Forest for Manifold Learning

The accuracy, scalability, and applicability of many machine learning algorithms is currently impeded by the high-dimensional and large-scale nature of most modern data sets. In particular, the dimensionality, or number of features, of many data sets is often high, often due to noise in the data – each data point is represented as a high-dimensional vector, but only a subset of them actually carries signals for subsequent inference. In other words, the data may lives near some unknown low-dimensional manifold embedded in some high-dimensional space. To gain a thorough understanding of the data, it is therefore often necessary to reduce its dimensionality in a way that preserves its underlying structure. *Manifold learning* is a set of tools designed to recover the underlying latent low-dimensional manifold structures of high-dimensional data.

Existing manifold learning methods, however, face a number of challenges. Linear approaches such as principal component analysis (PCA) Pearson [1901], independent component analysis (ICA) Hyvärinen and Oja [2000], canonical correlation analysis (CCA) Hotelling [1936], multidimensional scaling (MDS)Cox and Cox [2000], CUR decompositions Mahoney and Drineas [2009], and Fisher's linear discriminant analysis (LDA), have been widely applied and useful in many domains, but make fairly strong assumptions of about a linear structure underlying a data set. To mitigate these

issues a number of methods that can be characterized as kernel PCA methods were devised Schölkopf et al. [1997], including Isomap Tenenbaum et al. [2000b], Laplacian eigenmaps Belkin and Niyogi [2002], maximum variance unfolding Weinberger and Saul [2006]. These approaches are quite fragile to algorithm parameters, and typically require $mathcalO(n^3)$ operations for n samples, which is prohibitively computationally expensive for many datasets. Methods based on exact nearest neighbors, such as t-Distributed Stochastic Neighbor Embedding (t-SNE) Maaten and Hinton [2008], and Uniform Manifold Approximation and Projection (UMAP) McInnes and Healy [2018] also suffer computationally for large n. Approximate nearest neighbor approaches can mitigate some of these computational issues. For example, Fast Approximate Nearest-Neighbor Matching (FLANN) Muja and Lowe [2014] is a popular algorithm for nearest-neighbor detection in high-dimensional data sets. But FLANN, like all the above mentioned manifold learning algorithms, always operates on the observed dimensionality of the data. When the true manifold is low-dimensional, and the data are high-dimensional, the additional noise dimensions will be problematic for any of these algorithms.

We there propose an approach that we dub *Unsupervised Randomer Forest* (URerF). Unlike the previously described methods, URerF does not need to compute geodesic distances between pairs of points. Instead, URerF examines local structure by recursively clustering data in a sparse linear subspace of the original data, building on the recently proposed randomer forest algorithm for supervised learning Tomita

et al. [2015]. This randomer forest approach allows URerF to separate meaningful structure in the data from the noise dimensions.

Another contribution of this manuscript is a novel method for evaluating manifold learning algorithms. Most existing manuscripts on the topic either embed the data into some low-dimensional space, such as 2D or 3D, and then merely visualize the results. This approach is obviously limited in a number of ways: (1) it is purely qualitative, (2) when the structure is higher dimensional it may be lost, and (3) it relies on an embedding, which introduces additional complications. Other manuscripts compare the results on some subsequent inference task, such as classification. Such an approach is only able to evaluate performance of the manifold learning algorithm composed with a particular subsequent inferential method, but not the manifold learning algorithm itself. We therefore introduce Precision@K, Recall@K, and Precision-Recall curves as quantitative metrics to evaluate manifold learning. The difference between our proposed metrics and standard metrics, is that we do not evalute nearest neighbors with respect to the high-dimensional observed data, but rather the true low-dimensional latent representations. If a manifold learning does poorly on this metric, it has no hope to perform well on subsequent tasks. Indeed Precision@k provides a theoretical bound on subsequent classification accuracy Devroye et al. [1997].

Chapter 2

Classical Multidimensional Scaling under Noise

2.1 Review of Classical Multidimensional Scaling

Given an $n \times n$ hollow symmetric dissimilarity matrix D, and an embedding dimension d, we seek $X \in \mathbb{R}^{n \times d}$, where the rows $X_1, X_2, \ldots, X_n \in \mathbb{R}^d$ of X represent coordinates of points in $\mathbb{R}^d$, such that the overall inter-point distances between X_i and X_j are as close as possible to the distances given by the dissimilarity matrix D. For a given matrix H, we shall denote by $H^{(2)} = H \circ H$ the element-wise squaring of the matrix H. Given D, classical multidimensional scaling involves the following

steps:

1. Compute the matrix $B = -\frac{1}{2}PD^{(2)}P$ where $P = I - 1_n 1_n^\top / n$ is the double centering matrix. Here I denotes the $n \times n$ identity matrix and $1_n = (1, \ldots, 1)^\top \in \mathbb{R}^n$.

2. Extract the d largest positive eigenvalues $s_1, \ldots, s_d$ of B and the corresponding eigenvectors $u_1, \ldots, u_d$.

3. Let $X = U_B S_B^{1/2} \in \mathbb{R}^{n \times d}$, where $U_B = (u_1, \ldots, u_d)$ and $S_B = \text{diag}(s_1, \ldots, s_d)$. Each row of X represents the coordinate of a point in $\mathbb{R}^d$.

In essence, the procedure minimizes the Strain loss function defined as $L(X) = \|XX^\top - B\|_F$ where $\|\cdot\|_F$ denote the Frobenius norm of a matrix. Furthermore, the resulting configuration X centers all points around the origin, resulting in an inherent issue of identifiability: X is unique only up to an orthogonal transformation. In the following presentation, we will write $X = U_B S_B^{1/2} W$ where W is some orthogonal matrix, for a suitably transformed X.

2.2 Noise Models and Embedding

2.2.1 Model 1: $\Delta^2 = D^2 + E$

In this section we propose three different but related noise models for the matrix of observed dissimilarities. Suppose that we have a latent or unobserved matrix D

of inter-point Euclidean distances between n points in $\mathbb{R}^d$, i.e. $D_{ij} = \|x_i - x_j\|$. Let $D^{(2)}$ denote the entry-wise square of D and Δ be the observed dissimilarity matrix, such as that measured via a scientific experiment.

The first noise model we consider is $\Delta^{(2)} = D^{(2)} + E$ where we think of $D^{(2)}$ as the signal matrix and E as the noise matrix; see also Zhang et al. [2016]. We shall assume that E satisfies the following conditions:

(i) $\mathbb{E}[E] = 0$, hence $\mathbb{E}[\Delta^{(2)}] = D^{(2)}$.

(ii) The matrix E is hollow and symmetric.

(iii) The entries E_{ij} are independent and $\mathrm{Var}(E_{ij}) = \sigma^2$.

(iv) There exists a finite constant C such that E_{ij} follows a sub-Gaussian distribution with variance proxy C for all i, j, i.e., $\mathbb{P}[E_{ij} \geq t] \leq 2\exp(-t^2/(2C))$ for all i, j.

2.2.2 Model 2: $\Delta = D + E$

The second error model we consider is $\Delta = D + E$. We once more require that the random matrix E satisfies conditions (i) to (iv) identical to that in the model $\Delta^{(2)} = D^{(2)} + E$ along with a constant third and fourth moment conditions, i.e., there exists finite constants γ and ξ such that (v) $\mathbb{E}[E_{ij}^3] \equiv \gamma$ and $\mathbb{E}[E_{ij}^4] \equiv \xi$ for all i, j.

2.2.3 Model 3: Matrix Completion

Finally, we consider a noise model where only a fraction of the entries of D are observed. More specifically, for a given $q \in [0, 1]$ let Δ be such that for $i < j$, with probability q we observe $\Delta_{ij} = D_{ij}$ and with probability $1 - q$, Δ_{ij} is unobserved in which case we set $\Delta_{ij} = 0$. We then have $\Delta = D + E$ where E_{ij} is distributed as $(-D_{ij}) \times \text{Bernoulli}(1 - q)$. Furthermore, $\mathbb{E}[\Delta] = q \cdot D$ and $E[\Delta^{(2)}] = q \cdot D^{(2)}$. This model is motivated by the widely-studied problems of distance matrix completion and sensor localization; see e.g., Alfakih et al. [1999], Chatterjee [2015], Javanmard and Montanari [2013], Patwari et al. [2005].

For each of the above noise models, we shall apply classical multidimensional scaling to the observed Δ to obtain a configuration matrix $\widehat{X}$ whose rows are the estimate of the latent, unobserved $X = [x_1, \ldots, x_n]^\top$. A natural question that arises is how the added noise affects the embedding configuration. That is, what is the relationship between the configuration X and $\widehat{X}$ obtained from classical multidimensional scaling of D and Δ ?

2.3 Related Works

The problem of recovering an Euclidean distance matrix from noisy or imperfect observations of pairwise dissimilarity scores arises naturally in many different contexts. For example, in Zhang et al. [2016], the authors considered the model

$\Delta^{(2)} = D^{(2)} + E$ along with the estimator

$$\widehat{D}^{(2)} = \underset{M \in \mathcal{D}_n^{(2)}}{\arg\max} \Big\{ \frac{1}{2} \|\Delta^{(2)} - M\|_F^2 + \lambda_n \text{trace } (-\frac{1}{2} PMP) \Big\}$$

for $D^{(2)}$. Here $\mathcal{D}_n^{(2)}$ is the set of $n \times n$ *squared* Euclidean distance matrix and λ_n is a tuning parameter. Corollary 6 in Zhang et al. [2016] states that under suitable model on E, with probability approaching to one we have

$$\|\widehat{D}^2 - D^2\|_F^2 \leq 36 n \sigma^2 (r+1) \tag{2.1}$$

where σ is the variance of the noise and r is the rank of D^2. In this paper we obtain, as a corollary of ours results, a bound of the same order on $\|\widehat{D}^2 - D^2\|_F^2$. Furthermore, our central limit theorem on the configuration matrix $\widehat{X}$ provides a more refined limiting result, albeit one of a different flavor from Eq. (2.1).

On the other hand, completing a distance matrix with missing entries has been a popular problem in the engineering and social sciences; see, for example, Alfakih et al. [1999], Bakonyi and Johnson [1995], Singer [2008], Spence and Domoney [1974] . Distance matrix completion is closely related to multidimensional scaling [Borg and Groenen, 2005, Chatterjee, 2015, Javanmard and Montanari, 2013, Oh et al., 2010]. Especially noteworthy is Theorem 2.5 of Chatterjee [2015], where the author established an upper bound for the mean squared error on the estimator $\widetilde{M}$ for a general distance matrix M. More specifically, let (K, d) be a compact metric space

and $x_1, \ldots, x_n$ be n arbitrary points in K. Let M be the $n \times n$ matrix whose ij-entry is $d(x_i, x_j)$. Let $\epsilon > 0$ be such that $q \geq n^{-1+\epsilon}$. For a given $\delta > 0$, let $N(\delta)$ be the covering number of K using balls of radius ϵ with respect to the metric d. Then there exists an estimator $\widetilde{M}$ obtained by truncating the singular value decomposition of M such that

$$\mathrm{MSE}(\widetilde{M}) \leq C \inf_{\delta > 0} \min\Big\{ \frac{\delta + \sqrt{N(\delta/4)/n}}{\sqrt{q}}, 1 \Big\} + C(\epsilon) e^{-ncq}$$

where c and C are constants depending on the truncation level η for the singular values of M and $C(\epsilon)$ is a constant depending only on ϵ and η. Of particular interest is the application of this theorem to the Euclidean distance matrix, for which we obtain roughly

$$\mathrm{MSE}(\widetilde{M}) \leq \frac{C n^{-1/3}}{\sqrt{q}}.$$

Another recent result for the configuration $\widehat{X}$ obtained from the incomplete distance matrix Δ is Theorem 1 of Taghizadeh [2014] which states that, with high probability

$$\|\widehat{X} - X\|_F \leq \mathcal{O}\Big(\frac{\sqrt{n}}{\sqrt{q}}\Big).$$

Our central limit theorem in this paper improves upon both results. It is worth mentioning that the Euclidean distance matrix completion problem can also be viewed from an optimization point of view. See Tasissa and Lai [2018] for a review of such approaches.

2.4 Main Theorems

Recall that a random variable X is sub-Gaussian if

$$\mathbb{P}[|X| > t] \leq 2e^{-\frac{t^2}{K^2}}$$

for some constant K and for all $t \geq 0$. Associated with a sub-Gaussian random variable X is a Orlicz norm defined as

$$\|X\|_{\psi_2} = \inf\{t > 0 : \mathbb{E}\exp(\frac{X^2}{t^2}) \leq 2\}.$$

A random vector X in $\mathbb{R}^n$ is called sub-Gaussian if the one-dimensional marginals $\langle X, x\rangle$ are sub-Gaussian random variables for all $x \in \mathbb{R}^n$, and the corresponding sub-Gaussian norm of X is defined as

$$\|X\|_{\psi_2} = \sup_{x \in S^{n-1}} \|\langle X, x\rangle\|_{\psi_2}.$$

We now present central limit theorems for the rows of the classical multidimensional scaling configuration $\widehat{X}$ for the three noise models in § 2.2.1. Intuitively speaking, the theorems established that the rows of $\widehat{X}$, after some orthogonal transformation, is approximately normally distributed around the rows of X. Furthermore, the covariance matrix will depend on the noise model and the true distribution of the points in the underlying space and are substantially different between the three

noise models considered. In particular, the covariance matrix for the noise model $\Delta^2 = D^2 + E$ in Theorem 2.4.1 depends only on the variance σ^2 of the noise E_{ij}. This is in contrast with the covariance matrices of the model $\Delta = D + E$ and the model $\mathbb{E}[\Delta] = qD$ in Theorem 2.4.3 and Theorem 2.4.4, both of which depend also on the underlying true distances D_{ij}. The machinery involved in proving these results are by and large the same and we refer the reader to the Appendix for a sketch of the proof. For ease of exposition, we denote by $(A)_i$ the i-th row of a matrix.

Theorem 2.4.1 (central limit theorem for $\Delta^2 = D^2 + E$) *Let $Z_1, \ldots, Z_n$ be independent and identically distributed according to a multivariate sub-Gaussian distribution F on $\mathbb{R}^d$. Let D be the Euclidean distance matrix generated by the Z_k's, i.e. $D_{ij} = \|Z_i - Z_j\|$. Let $\Delta^2 = D^2 + E$ where the noise matrix E satisfy the conditions (i) $\mathbb{E}[E] = \mathbf{0}$, (ii) E is hollow and symmetric, (iii) the entries E_{ij} are independent for $i \leq j$ with $\mathrm{Var}[E_{ij}] \equiv \sigma^2$, and (iv) each E_{ij} follows a sub-Gaussian distribution. Denote by $\widehat{X}_n$ the classical multidimensional scaling embedding configurations of Δ into $\mathbb{R}^d$. There exists a sequence of $d \times d$ orthogonal matrices $\{W_n\}_{n=1}^{\infty}$ such that for any $\alpha \in \mathbb{R}^d$ and any fixed row index i, we have*

$$\lim_{n\to\infty} \mathbb{P}\{n^{1/2}[(\widehat{X}_n W_n)_i - (Z_i - \bar{Z})] \leq \alpha\} = \Phi(\alpha, \Sigma)$$

where $\bar{Z}$ is the mean of Z_k's and $\Phi(\alpha, \Sigma)$ denotes the cumulative distribution function of a multivariate Gaussian with mean 0 and covariance matrix Σ, evaluated at α.

Here $\Sigma = \frac{\sigma^2}{4}\Xi^{-1}$ *where* $\Xi = \mathrm{cov}(Z_k) \in \mathbb{R}^{d\times d}$.

Remark 2.4.2 *We can relax the common variance requirement (iii) in Theorem 2.4.1. Let* $Var(E_{ij}) = \sigma_{ij}^2$ *and suppose that, for a fixed* i*, the collection* $(D_{ij}^2 - \Delta_{ij}^2)(Z_j - \mathbb{E}[Z_j])$ *for* $j \neq i$ *satisfies the conditions for the Lindeberg-Feller central limit theorem. Let* $\Sigma_i = n^{-1}\sum_j \sigma_{ij}^2 \mathrm{cov}(Z_k)$*. We obtain the following variant of Theorem 2.4.1:*

$$n^{1/2}\Sigma_i^{-\frac{1}{2}}\big((\widehat{X_n W_n})_i - (Z_i - \bar{Z})\big) \to \mathcal{N}(0, I).$$

Theorem 2.4.3 (Central Limit Theorem for $\Delta = D + E$**)** *Let* $Z_1, \ldots, Z_n$ *be independent and identically distributed according to a multivariate sub-Gaussian distribution* F *on* $\mathbb{R}^d$*. Let* D *be the Euclidean distance matrix generated by the* Z_k*'s, i.e.* $D_{ij} = \|Z_i - Z_j\|$*. Let* $\Delta = D + E$ *and suppose that the noise matrix* E *satisfy, in addition to the conditions in Theorem 2.4.1, the condition (v)* $\mathbb{E}[E_{ij}^3] \equiv \gamma$ *and* $\mathbb{E}[E_{ij}^4] \equiv \xi$*. Denote by* $\widehat{X}_n$ *the classical multidimensional embedding of* Δ *into* $\mathbb{R}^d$*. There exists a sequence of* $d \times d$ *orthogonal matrices* $\{W_n\}_{n=1}^{\infty}$ *such that for any* $\alpha \in \mathbb{R}^d$ *and any fixed row index* i*,*

$$\lim_{n\to\infty} \mathbb{P}\{n^{1/2}\big((\widehat{X}_n W_n)_i - (Z_i - \bar{Z})\big) \leq \alpha\} = \int \Phi(\alpha, \Sigma(z))dF(z)$$

where $\bar{Z}$ *is the mean of* Z_k*'s and* $\Phi(\alpha, \Sigma)$ *denotes the cumulative distribution function of a multivariate Gaussian with mean* 0 *and covariance matrix* Σ*, evaluated at* α*.*

Here $\Sigma(z) = \Xi^{-1}\widetilde{\Sigma}(z)\Xi^{-1}$ *where* $\Xi = \mathrm{cov}(Z_i) \in \mathbb{R}^{d\times d}$ *and, with* $\mu = \mathbb{E}[Z_i] \in \mathbb{R}^d$,

$$\widetilde{\Sigma}(z) = \mathbb{E}_{Z_k}\Big[(\sigma^2\|z - Z_k\|^2 + \gamma\|z - Z_k\| + \frac{1}{4}\xi - \frac{\sigma^4}{4})(Z_k - \mu)(Z_k - \mu)^\top\Big]$$

is a covariance matrix depending on z.

Theorem 2.4.4 (Central Limit Theorem for $\Delta = D$ with missing entries) *Let* $Z_1, \ldots, Z_n$ *be independent and identically distributed according to a multivariate sub-Gaussian distribution* F *on* $\mathbb{R}^d$. *Let* D *be the Euclidean distance matrix generated by the* Z_i*'s, i.e.* $D_{ij} = \|Z_i - Z_j\|$. *Suppose that with probability* $q_n \in [0, 1]$ *we observe the distance* D_{ij} *and with probability* $1 - q_n$ *it is missing, i.e.,* $\Delta = D + E$ *where* $E_{ij} = (-D_{ij}) \times \mathrm{Bernoulli}(1 - q_n)$. *Denote by* $\widehat{X}_n$ *the classical multidimensional embedding of* Δ *into* $\mathbb{R}^d$. *Then there exists a sequence of* $d \times d$ *orthogonal matrices* $\{W_n\}_{n=1}^{\infty}$ *such that if* $nq_n = \omega(\log^4 n)$, *then for any* $\alpha \in \mathbb{R}^d$ *and any fixed row index* i,

$$\lim_{n\to\infty} \mathbb{P}\{n^{1/2}[(\widehat{X_n}W_n)_i - q_n^{1/2}(Z_i - \bar{Z})] \le \alpha\} = \int \Phi(\alpha, \Sigma(z))dF(\mathrm{z})$$

where $\bar{Z}$ *is the mean of* Z_i*'s and* $\Phi(\alpha, \Sigma)$ *denotes the CDF of a multivariate Gaussian with mean* 0 *and covariance matrix* Σ, *evaluated at* α. *Here* $\Sigma(z) = \Xi^{-1}\widetilde{\Sigma}(z)\Xi^{-1}$, $\Xi = \mathrm{cov}(Z_i) \in \mathbb{R}^{d\times d}$ *and with* $\mu = \mathbb{E}[Z_i] \in \mathbb{R}^d$,

$$\widetilde{\Sigma}(z) = \frac{1 - q_n}{4} \times \mathbb{E}_{Z_k}\Big[\|z - Z_k\|^4(Z_k - \mu)(Z_k - \mu)^\top\Big]$$

is a covariance matrix depending on z.

Remark 2.4.5 *We emphasize that, in the statement of Theorem 2.4.4, $(\widehat{X_n}W_n)_i$ is centered around $q_n^{1/2}(Z_i - \bar{Z})$ and not around $Z_i - \bar{Z}$. Therefore, unless q_n is known or that an identifiability condition is specified, the classical multidimensional scaling configuration $\widehat{X}_n$ will only recovers an estimate of $Z - 1_n\bar{Z}$ up to an orthogonal transformation W_n and a scaling factor $q_n^{1/2}$.*

2.5 Empirical Results

2.5.1 Three Point-mass Simulated Data

As a simple illustration of our central limit theorem, we embed noisy Euclidean distances obtained from n points into $\mathbb{R}^2$. For illustrative purpose, we will focus on the error model $\Delta = D + E$ as in Theorem 2.4.3. Experimental results for the other error models are completely analogous. We consider three points $x_1, x_2, x_3 \in \mathbb{R}^2$ for which the inter-point distances are 3,4 and 5 (these three points form a right triangle) and generate $n_k = \pi_k n$ points equal to x_k, $k = 1, 2, 3$, where $\pi = [0.2, 0.3, 0.5]^\top$. The resulting Euclidean inter-point distance matrix D is then subjected to uniform noise, yielding $\Delta = D + E$ where $E_{ij} \overset{i.i.d.}{\sim} \text{Uniform}(-4, +4)$ for $i < j$ and $E_{ij} = E_{ji}$. For this setting, our central limit theorem for the classical multidimensional embedding of Δ into $\mathbb{R}^2$ yields class-conditional Gaussians. For $n \in \{50, 100, 1000\}$, Figure 2.1

	n=50	n=100	n=500	n=1000
$\widehat{\Sigma}^{(1)}$:	$\begin{bmatrix} 14.15 & 0.25 \\ 0.25 & 79.07 \end{bmatrix}$	$\begin{bmatrix} 13.67 & -0.79 \\ -0.79 & 98.96 \end{bmatrix}$	$\begin{bmatrix} 13.65 & -2.34 \\ -2.34 & 41.02 \end{bmatrix}$	$\begin{bmatrix} 13.63 & -2.70 \\ -2.70 & 31.76 \end{bmatrix}$
$\text{Var}\begin{bmatrix} \widehat{\Sigma}^{(1)}_{11} \\ \widehat{\Sigma}^{(1)}_{12} \\ \widehat{\Sigma}^{(1)}_{22} \end{bmatrix}$:	$\begin{bmatrix} 41.25 \\ 113.31 \\ 829.52 \end{bmatrix}$	$\begin{bmatrix} 19.29 \\ 68.06 \\ 984.45 \end{bmatrix}$	$\begin{bmatrix} 3.67 \\ 7.87 \\ 31.71 \end{bmatrix}$	$\begin{bmatrix} 1.71 \\ 3.25 \\ 11.08 \end{bmatrix}$

Table 2.1: Empirical average of covariance matrix $\widehat{\Sigma}^{(1)}$, and entry-wise variance (500 simulations).

compares, for one realization, the theoretical vs. estimated means and covariances matrices (95% level curves). Table 2.1 shows the empirical covariance matrix for one of the point masses, $\widehat{\Sigma}^{(1)}$, behaving in accordance with Theorem 2.4.3.

Table 2.1 investigates the empirical covariance matrix for one of the point masses, and its entry-wise variance, as a function of n. The theoretical covariance matrix is

$$\Sigma^{(1)} = \begin{bmatrix} 13.56 & -3.06 \\ -3.06 & 22.65 \end{bmatrix}$$

Remark 2.5.1 *In this simulation we relax the requirement that the entries of* Δ *should be nonnegative in order to illustrate the phenomenon of decreasing covariance with increasing* n*.*

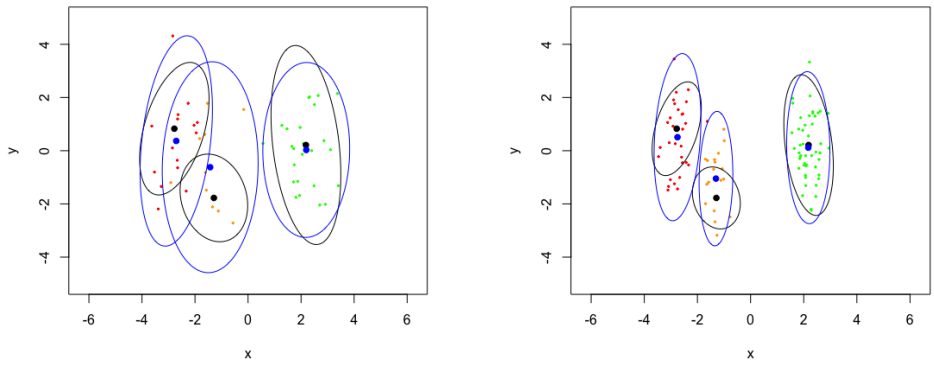

(a) n=50 **(b)** n=100

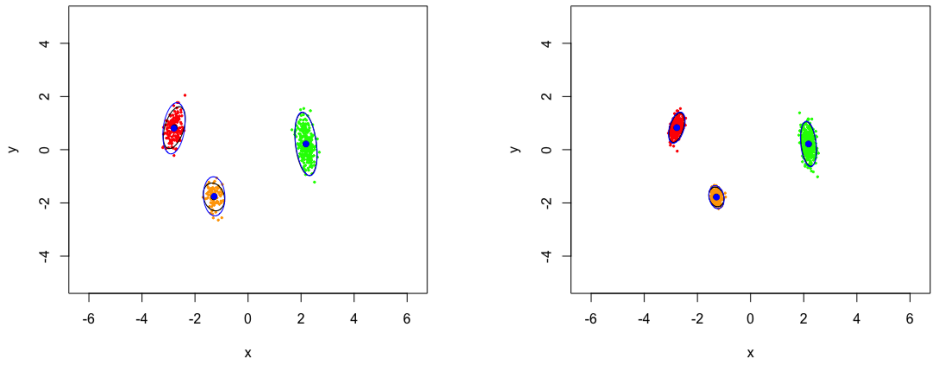

(c) n=500 **(d)** n=1000

Figure 2.1: Simulation results for n=50, 100, 500 and 1000 points, as described in Section 2.5.1. The blue ellipses are the 95% level curves of the empirical covariance matrix, and the blue dots are the empirical centers for three classes. The black dots are the true positions of x_1, x_2 and x_3, and the black ellipses are the 95% level curve for the theoretical covariance matrices as in Theorem 2.4.3. Note that the blue and black centers and ellipses coincide for large n.

2.5.2 Shape clustering

As a second illustration of the effect of noise on CMDS, we examine a more involved clustering experiment in the (non-Euclidean) shape space of closed curves. In this experiment, we consider boundary curves obtained from silhouettes of the Kimia shape database. Specifically, we restrict attention to three predefined classes of objects (bottle, bone, and wrench) and take from each class three different examples of shapes all given by planar closed polygonal curves representing the objects' outline. Figure 2.2 shows one instance for each of the bottle, bone, and wrench class. A database of noisy curves is then created as follows: for each of the nine template shapes, we generate 100 noisy realizations in which vertices of the curve are moved along the curve's normal vectors with random distances drawn from independent Gaussian distributions at each vertex. This results in a total of 900 noisy versions of the initial curves such as the ones displayed in Figure 2.3.

(a) Bottle **(b)** Bone **(c)** Wrench

Figure 2.2: Examples from the Kimia Dataset.

We then compute the pairwise distance matrix between all the curves (including the noiseless templates) based on a shape distance which was introduced in Glaunès

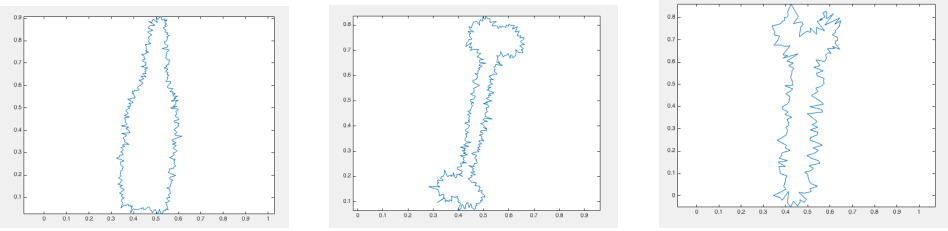

(a) Bottle **(b)** Bone **(c)** Wrench

Figure 2.3: Noisy versions of examples from the Kimia Dataset.

et al. [2008] and later extended in the work of Kaltenmark et al. [2017]. This type of metric is based on the representation of shapes in a particular distribution space called currents, see Kaltenmark et al. [2017] for details. In our context, this metric offers several advantages: (i) the distance is completely geometrical in the sense that it is independent of the sampling of the curves and does not rely on predefined pointwise correspondences between vertices; (ii) it has an intrinsic smoothing effect that provides robustness to noise to a certain degree; (iii) it can be computed in closed form with minimal computational time which is critical given the large number of pairwise distances to evaluate. In this setting, we can view the resulting distance matrix as a perturbation of the ideal distances between the 9 template curves, which fits into the generic framework of our model. (Note that we leave aside the issue of checking the technical assumptions on the matrix E, which may be quite involved for this noise model and distance.)

We proceed to perform CMDS on this distance matrix. A scree plot investigation shows that an appropriate embedding dimension here is $\widehat{d} = 3$ (the top three eigenvalues are 2.20, 0.68, 0.06 with the fourth $\ll 0.01$). The resulting embedding config-

uration is shown in Figure 2.4. This configuration exhibits nine fairly well-separated clusters roughly centered around the position of each of the noiseless template curves. Those, in turn, form 3 'super-clusters' consistent with the classes. Furthermore, the ellipsoidal shape of each cluster suggests that the configuration approximately follows a Gaussian distribution.

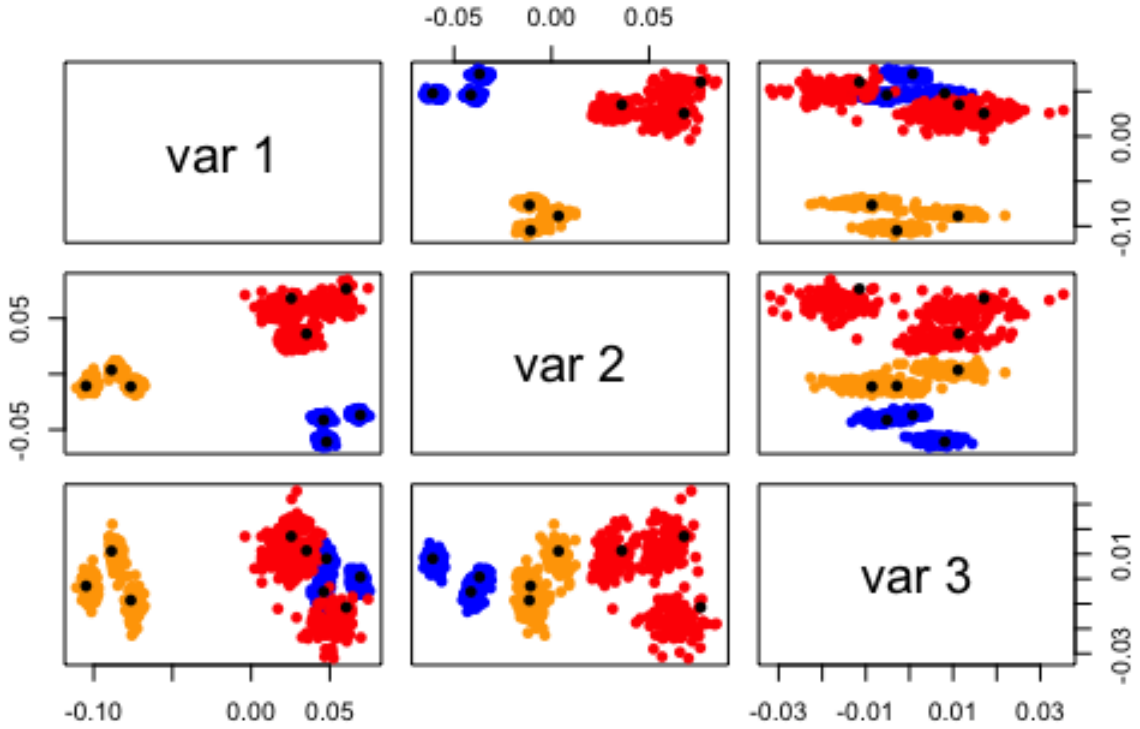

Figure 2.4: Pairs plot of CMDS into $\mathbb{R}^3$ for the noisy curves. Colors correspond to the different classes (blue for bottle, red for bone, and orange for wrench). The position of the nine template curves in the configuration are highlighted with large black dots.

While these preliminary shape clustering results are obtained with a specific and simple distance on the space of curves, future work will investigate whether similar

properties hold with different, more elaborate metrics and/or geometric noise models. The central limit theorem derived here could then constitute a useful theoretical tool to evaluate the discriminating power of shape clustering methods based on CMDS.

2.6 Discussion

In Athreya et al. [2016] and Levin et al. [2017], the authors prove that adjacency spectral embedding of the random dot product graph gives rise to a central limit theorem for the estimated latent positions. In this work we extend these results to the previously unexplored area of perturbation analysis for CMDS, addressing a gap in the literature as acknowledged in Fan et al. [2018] and Peterfreund and Gavish [2018]. Notably, the three noise models we proposed in Section 2.2.1 each give rise to a central limit theorem; that is, for Euclidean distance matrix, the rows of the configuration matrix given by CMDS under noise will center around the corresponding rows of the true configuration matrix. Furthermore, our simulations on the synthetic data together with the shape clustering data all demonstrated the validity of our results. We have avoided any discussion of the model selection problem of choosing a suitable embedding dimension $\widehat{d}$. Instead, we assume d is known – except in Section 4.2. There are many methods for choosing (spectral) embedding dimensions, see Chatterjee [2015], Jackson [1991], Zhu and Ghodsi [2006].

A practically relevant and conceptually illustrative example comes from relaxing

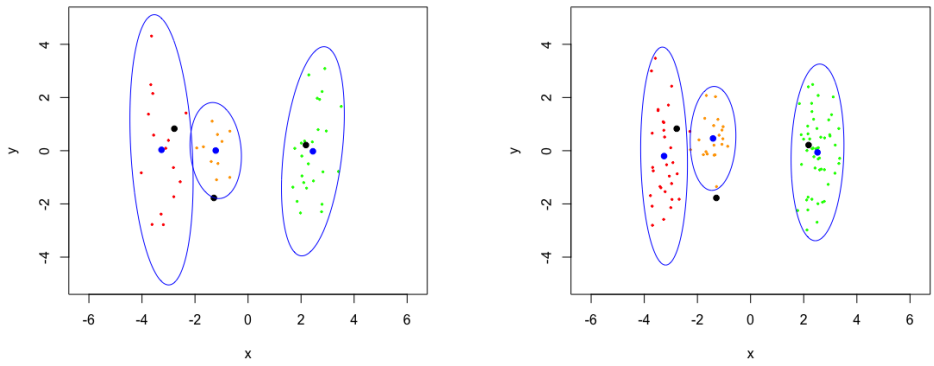

(a) n=50 **(b)** n=100

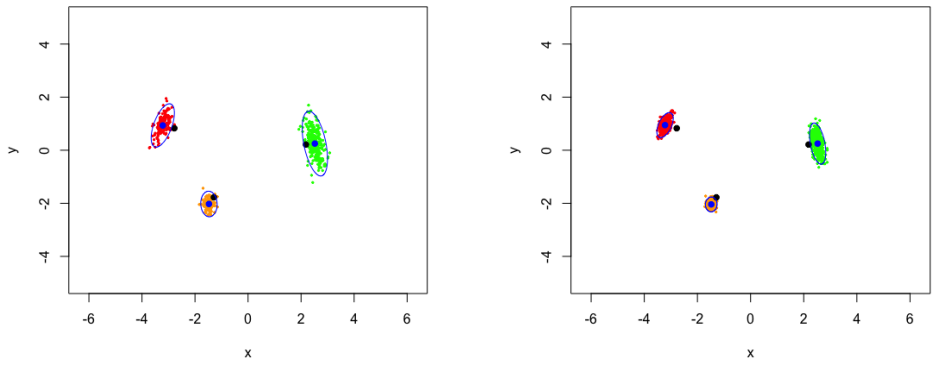

(c) n=500 **(d)** n=1000

Figure 2.5: Simulation of CMDS with heteroscedastic noise $\widetilde{E}$. The black dots are the true positions for the three points. The blue dots are the empirical means and the blue ellipses are the 95% level curve of the empirical covariance matrix. Note that $\widetilde{E}$ used in this simulation is of the same order for the off-diagonal blocks as that used in Figure 2.1. NB: there is asymptotic bias.

the assumption of common variance for the entries of the noise matrix E in Section 2.2.2: the consistency result from Theorem 2.4.3 no longer holds. To illustrate this point, we return to our three-point-mass simulation presented in Section 2.5.1 and modify our noise model as follows: Let $\widetilde{E}_{ij} \overset{i.i.d.}{\sim} \text{Uniform}(-D_{ij}, +D_{ij})$ for $i < j$ and $\widetilde{E}_{ij} = \widetilde{E}_{ji}$. (The noise now depends on the entries of D, and $\Delta = D + \widetilde{E}$ no longer has negative entries.) The embedding of Δ into two dimensions gives class-conditional Gaussians; however, we have introduced bias into the embedding configuration. Figure 2.5 shows, for one realization, the embedding result. Note that the empirical mean and the theoretical positions do not coincide in simulation with large n, and theoretically even in the limit.

CMDS is just one of a wide variety of multidimensional scaling techniques. Minimizing the raw stress criterion is another commonly used MDS technique [de Leeuw and Heiser, 1982], i.e., given a $n \times n$ observed dissimilarity matrix Δ and an embedding dimension d, one seeks to minimize the objective function

$$\sigma_r = \sigma_r(X) = \sum_{(i,j)} (\delta_{ij} - \|X_i - X_j\|)^2.$$

The minimization of $\sigma_r(X)$ is with respect to all configurations $X \in \mathbb{R}^{n \times d}$ and usually proceeds via an iterative algorithm which updates the configuration matrix X until a stopping criterion is met. Keeping the simulation settings as in Section 2.5.1, the resulting configuration is shown in Figure 2.6. This suggests that the CLT may hold

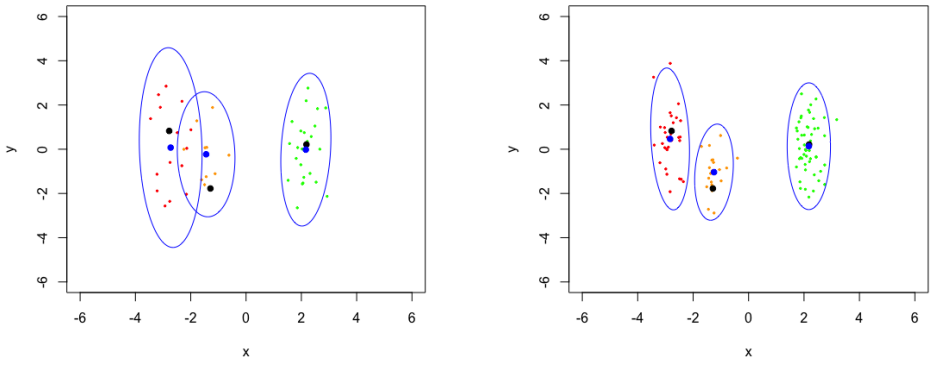

(a) n=50 **(b)** n=100

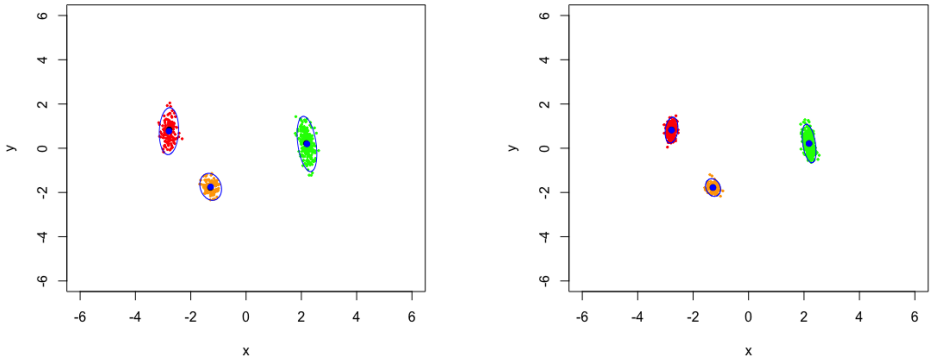

(c) n=500 **(d)** n=1000

Figure 2.6: Simulation of MDS using raw stress criterion for n=50, 100, 500 and 1000 points. The black dots are the true positions of x_1, x_2 and x_3, the blue dots are the empirical mean of the simulation and the blue ellipses are the 95% level curve of the empirical covariance matrix.

for raw stress just as well as for CMDS. However, this claim is at best a conjecture at present as perturbation analysis of stress minimization algorithms is significantly more involved.

2.7 Conjecture: CMDS on Omni Embedding of graphs and Hypothesis Testing

Given a collection of Random Dot Product Graphs: $A^{(1)}, A^{(2)}, \ldots, A^{(m)}$, each with n vertices, Levin et al. [2017] seeks to jointly embed all m graphs into a common (prespecified) d-dimensional Euclidean space by embedding the $nm \times nm$ OMNI Matrix $\mathcal{M}$ given by

$$\mathcal{M} := \begin{bmatrix} A^{(1)} & \frac{A^{(1)}+A^{(2)}}{2} & \frac{A^{(1)}+A^{(3)}}{2} & \ldots & \frac{A^{(1)}+A^{(m)}}{2} \\ \frac{A^{(2)}+A^{(2)}}{2} & A^{(2)} & \frac{A^{(2)}+A^{(3)}}{2} & \ldots & \frac{A^{(2)}+A^{(m)}}{2} \\ \vdots & \vdots & \vdots & \ldots & \vdots \\ \frac{A^{(m)}+A^{(1)}}{2} & \frac{A^{(m)}+A^{(2)}}{2} & \frac{A^{(m)}+A^{(3)}}{2} & \ldots & A^{(m)} \end{bmatrix}.$$

Using the notation in Levin et al. [2017], let $S_{\mathcal{M}}$ represent the $d \times d$ matrix of top d eigenvalues of $\mathcal{M}$, ordered by magnitude, and let $U_{\mathcal{M}}$ be the $mn \times d$-dimensional matrix of associated eigenvectors. Define the omnibus embedding, denoted OMNI($\mathcal{M}$),

by $U_{\mathcal{M}} S_{\mathcal{M}}^{1/2}$, note that OMNI($\mathcal{M}$) produces m separate points in Euclidean for each graph vertex, effectively one such point for each copy of the multiple graphs in our sample. Furthermore, denote

$$U_{\mathcal{M}} S_{\mathcal{M}}^{1/2} = \begin{bmatrix} \widehat{X}^{(1)} \\ \widehat{X}^{(2)} \\ \vdots \\ \widehat{X}^{(m)} \end{bmatrix} \tag{2.2}$$

where each $\widehat{X}^{(i)}$ is an $n \times d$ matrix representing the embedding of the ith random graph in d dimension.

As pointed out in Levin et al. [2017], the omnibus embedding introduces alignment between graphs by placing an average on the off-diagonal blocks of $\mathcal{M}$, merely considering a Frobenius norm difference between blocks of the omnibus embedding $\|\widehat{X}^{(i)} - \widehat{X}^{(j)}\|_F$ without any Procrustes alignments provides meaningful discrimination between graphs with different latent positions. Specifically, we can construct an $m \times m$ distance matrix Δ given by $\Delta_{ij} := \|\widehat{X}^{(i)} - \widehat{X}^{(j)}\|_F$ as an estimation for the Frobenius distance matrix D between true latent positions $D_{ij} := \|X^{(i)} - X^{(j)}\|_F$, where $X^{(i)}$ is the true latent position for the ith graph. That is, $\Delta = D + E$ for some $m \times m$ noise matrix E. (Note that the entries of E are correlated. Furthermore, $\mathbb{E}[E] = 0$ only when all the m graphs shares the same underlying true latent position. Those two observations make the proof of the following conjectures quite a bit more

challenging).

A natural thing to do now is to perform classical multidimensional scaling (CMDS) on Δ and D and compare the resulting configuration matrix $\widehat{\mathcal{G}}$ = CMDS(Δ) and $\mathcal{G}$ = CMDS(D), and we propose the following conjecture:

Conjecture 2.7.1 *Using the above notations, we propose:*

$$\lim_{m\to\infty} \mathbb{P}\{\sqrt{m}[(\widehat{\mathcal{G}}W_m)_i - (\mathcal{G})_i] \leq \alpha\} = \int_{suppF} \Phi(\alpha, \Sigma(\mathrm{z}))dF(\mathrm{z})$$

where z's depends on the true underlying distribution of the latent positions X of the graphs.

2.8 Proof of the Theorems

2.8.1 Proof of Theorem 2.4.3

We proceed to give a complete proof for Theorem 2.4.3. Theorems 2.4.1 and 2.4.4 will have different covariance matrix structures then what is given in Lemma 2.8.3 and will be dealt with later.

Given a matrix A, we denote by $\|A\|$ and $\|A\|_F$ its spectral and Frobenius norm, respectively. We will utilize the following observation repeatedly in our presentation.

Observation 2.8.1 *Let A and B be matrices of appropriate dimensions. Then*

$$\|AB\|_F = \|B^\top A^\top\|_F \leq \min\{\|A\| \times \|B\|_F, \|B\| \times \|A\|_F\}.$$

We remind our readers the following notations for the subsequent presentation. Recall that

$$B = -\tfrac{1}{2} P D^{(2)} P$$

and

$$\widehat{B} = -\frac{1}{2} P \Delta^{(2)} P$$

are the double centering of $D^{(2)}$ and $\Delta^{(2)}$, respectively. If $D^{(2)}$ is a Euclidean distance matrix whose elements are $D_{ij} = \|Z_i - Z_j\|$, then

$$B = PZZ^\top P.$$

In particular,

$$U_B S_B^{1/2} = PZ\widetilde{W}$$

for some $d \times d$ orthogonal matrix $\widetilde{W}$. The ith row of $U_B S_B^{1/2}$ is then $\widetilde{W}_n^\top (Z_i - \bar{Z})$. Now let W^* be the orthogonal matrix satisfying

$$W^* = \arg\min_W \|U_B^\top U_{\widehat{B}} - W\|_F.$$

The following lemma provides a decomposition for $\widehat{X} - U_B S_B^{1/2} W^*$ into a sum of several matrices.

Lemma 2.8.2 *Let W^* be the orthogonal matrix satisfying*

$$W^* = \arg\min_W \|U_B^\top U_{\widehat{B}} - W\|.$$

Then

$$\begin{aligned}
\widehat{X} - U_B S_B^{1/2} W^* =& (\widehat{B} - B) U_B S_B^{-1/2} W^* && (2.3)\\
&- (\widehat{B} - B) U_B (S_B^{-1/2} W^* - W^* S_{\widehat{B}}^{-1/2}) - U_B U_B^\top (\widehat{B} - B) U_B W^* S_{\widehat{B}}^{-1/2} && (2.4)\\
&+ (I - U_B U_B^\top)(\widehat{B} - B)(U_{\widehat{B}} - U_B W^*) S_{\widehat{B}}^{-1/2} && (2.5)\\
&+ U_B (U_B^\top U_{\widehat{B}} - W^*) S_{\widehat{B}}^{1/2} + U_B (W^* S_{\widehat{B}}^{1/2} - S_B^{1/2} W^*) && (2.6)
\end{aligned}$$

Proof: We have

$$\begin{aligned}
\widehat{X} - U_B S_B^{1/2} W^* =& U_{\widehat{B}} S_{\widehat{B}}^{1/2} - U_B W^* S_{\widehat{B}}^{1/2} + U_B (W^* S_{\widehat{B}}^{1/2} - S_B^{1/2} W^*) \\
=& U_{\widehat{B}} S_{\widehat{B}}^{1/2} - U_B U_B^\top U_{\widehat{B}} S_{\widehat{B}}^{1/2} + U_B U_B^\top U_{\widehat{B}} S_{\widehat{B}}^{1/2} - U_B W^* S_{\widehat{B}}^{1/2} \\
&+ U_B (W^* S_{\widehat{B}}^{1/2} - S_B^{1/2} W^*) \\
=& (I - U_B U_B^\top) \widehat{B} U_{\widehat{B}} S_{\widehat{B}}^{-1/2} + U_B (U_B^\top U_{\widehat{B}} - W^*) S_{\widehat{B}}^{1/2} + U_B (W^* S_{\widehat{B}}^{1/2} - S_B^{1/2} W^*) \\
=& (I - U_B U_B^\top)(\widehat{B} - B) U_{\widehat{B}} S_{\widehat{B}}^{-1/2} \\
&+ U_B (U_B^\top U_{\widehat{B}} - W^*) S_{\widehat{B}}^{1/2} + U_B (W^* S_{\widehat{B}}^{1/2} - S_B^{1/2} W^*).
\end{aligned}$$

We used the facts $U_B U_B^\top B = B$ and $U_{\widehat{B}} S_{\widehat{B}}^{1/2} = \widehat{B} U_{\widehat{B}} S_{\widehat{B}}^{-1/2}$ in the above equalities. The last two terms of the above display is Eq. (2.6). Denote

$$R := (I - U_B U_B^\top)(\widehat{B} - B) U_{\widehat{B}} S_{\widehat{B}}^{-1/2},$$

we then have

$$\begin{aligned}
R =& (I - U_B U_B^\top)(\widehat{B} - B)(U_B W^* + U_{\widehat{B}} - U_B W^*) S_{\widehat{B}}^{-1/2} \\
=& (\widehat{B} - B) U_B W^* S_{\widehat{B}}^{-1/2} - U_B U_B^\top (\widehat{B} - B) U_B W^* S_{\widehat{B}}^{-1/2} \\
&+ (I - U_B U_B^\top)(\widehat{B} - B)(U_{\widehat{B}} - U_B W^*) S_{\widehat{B}}^{-1/2} \\
=& (\widehat{B} - B) U_B S_B^{-1/2} W^* - (\widehat{B} - B) U_B (S_B^{-1/2} W^* - W^* S_{\widehat{B}}^{-1/2}) \\
&- U_B U_B^\top (\widehat{B} - B) U_B W^* S_{\widehat{B}}^{-1/2} + (I - U_B U_B^\top)(\widehat{B} - B)(U_{\widehat{B}} - U_B W^*) S_{\widehat{B}}^{-1/2}
\end{aligned}$$

The four terms in the above display are identical to that in Eq. (2.3) through Eq. (2.5).

■

Lemma 2.8.2 implies

$$\widehat{X}W^{*\top}\widetilde{W}_n - U_B S_B^{1/2}\widetilde{W}_n = \widehat{X}W^{*\top}\widetilde{W}_n - PZ = (\widehat{B} - B)U_B S_B^{-1/2}\widetilde{W}_n + R_n\widetilde{W}_n$$

where R_n are the matrices in Eq. (2.4) through Eq. (2.6). The essential term is

$$(\widehat{B} - B)U_B S_B^{-1/2}\widetilde{W}_n.$$

We analyzed the rows of this matrix in Lemma 2.8.3 where we show that they converge to multivariate normals. Meanwhile, Lemma 2.8.4 shows that the rows of the matrices R_n, when scaled by $n^{1/2}$, converge to 0 in probability. Combining these results yield Theorem 2. A few minor changes to the covariance computation in the proof of Lemma 2.8.3 also yield Theorem 2.4.1 and Theorem 2.4.4.

Lemma 2.8.3 *Let $Z_1, \ldots, Z_n$ be independent and identically distributed according to some multivariate sub-Gaussian distribution F. Then there exists a sequence of $d \times d$ orthogonal matrices $\widetilde{W}_n$, such that for any fixed index i with $Z_i = z_i$, we have*

$$n^{1/2}\widetilde{W}_n^{\top}[(\widehat{B} - B)U_B S_B^{-1/2}]_i \longrightarrow \mathcal{N}(0, \Sigma(z_i))$$

where $\Sigma(z_i) = \Xi^{-1}\widetilde{\Sigma}(z_i)\Xi^{-1}$, $\Xi = \mathbb{E}[Z_k {Z_k}^\top] \in \mathbb{R}^{d\times d}$, $\mu = \mathbb{E}[Z_k] \in \mathbb{R}^d$ *and*

$$\widetilde{\Sigma}(z_i) = \mathbb{E}_{Z_k}[(\sigma^2\|z_i - Z_k\|^2 + \mathbb{E}[E_{ij}^3]\|z_i - Z_k\| + \frac{1}{4}\mathbb{E}[E_{ij}^4] - \frac{\sigma^4}{4})(Z_k - \mu)(Z_k - \mu)^\top] \in \mathbb{R}^{d\times d}$$

is a covariance matrix depending on z. *Here* $(A)_i$ *or* $[A]_i$ *denote the* i*th row of a matrix* A.

Proof: Recall that $PZ = U_B S_B^{1/2}\widetilde{W}_n$. We therefore have

$$\begin{aligned}
n^{1/2}\widetilde{W}_n^\top[(\widehat{B} - B)U_B S_B^{-1/2}]_i &= n^{1/2}\widetilde{W}_n^\top[(\widehat{B} - B)PZ\widetilde{W}_n^\top {S_B}^{-1}]_i \\
&= n^{1/2}\widetilde{W}_n^\top {S_B}^{-1}\widetilde{W}_n[(\widehat{B} - B)PZ]_i \\
&= -n^{1/2}\widetilde{W}_n^\top {S_B}^{-1}\widetilde{W}_n[P(D\circ E + \frac{E^2}{2})PZ]_i \\
&= -n^{1/2}\widetilde{W}_n^\top {S_B}^{-1}\widetilde{W}_n\Big[P\Big(D\circ E + \frac{E^2 - \sigma^2 1_n 1_n^\top}{2}\Big)PZ\Big]_i
\end{aligned}$$

The last equality holds since $P1_n = 0$. Now

$$PZ = Z - 1_n\bar{Z} = Z - 1_n\mu^\top + \widetilde{R}_n$$

where $\|\widetilde{R}_n\| = O(n^{-1/2})$ with high probability. Therefore,

$$\begin{aligned}
n^{1/2}\widetilde{W}_n^\top[(\widehat{B} - B)U_B S_B^{-1/2}]_i = &- n\widetilde{W}_n^\top S_B^{-1}\widetilde{W}_n\Big[n^{-1/2}\sum_{j\neq i}^{n}\Big(D_{ij}E_{ij} + \frac{E_{ij}^2 - \sigma^2 1_n 1_n^\top}{2}\Big)(Z_j - \mu)\Big] \\
&+ o(1)
\end{aligned}$$

Conditioning on $Z_i = z_i$ and ignoring the term $o(1)$ that vanishes as $n \to \infty$, the above expression is sum of $n-1$ independent mean 0 random vector. We then invoke the Lindeberg-Feller central limit theorem to show that this sum converges to a multivariate normal. We now evaluate the covariance matrix for this sum. Each summand has covariance matrix of the form

$$\mathrm{cov}[(E_{ij}D_{ij} + \frac{E_{ij}^2 - \sigma^2}{2})(Z_j - \mu)] = \mathrm{Var}\Big(E_{ij}\|z_i - Z_j\| + \frac{E_{ij}^2 - \sigma^2}{2}\Big)(Z_j - \mu)(Z_j - \mu)^\top.$$

Since $\mathbb{E}[E_{ij}] = 0$ and $\mathbb{E}[E_{ij}^2] = \sigma^2$, we also have

$$\mathrm{Var}\Big(E_{ij}\|z_i - Z_j\| + (E_{ij}^2 - \sigma^2)/2\Big) = \mathbb{E}\Big[E_{ij}^2\|z_i - Z_j\|^2 + E_{ij}\|z_i - Z_j\|(E_{ij}^2 - \sigma^2) + \frac{(E_{ij}^2 - \sigma^2)^2}{4}\Big]$$

where the expectation is taken with respect to E_{ij} and conditional on Z_j. Averaging over the indices j and then taking the limit as $n \to \infty$ yields

$$\begin{aligned}\widetilde{\Sigma}_n(z_i) &= \mathrm{Var}\Big[n^{-1/2}\sum_{j\neq i}^{n}\Big(D_{ij}E_{ij} + \frac{E_{ij}^2 - \sigma^2 1_n 1_n^\top}{2}\Big)(Z_j - \mu)\Big] \\ &\longrightarrow \mathbb{E}_{Z_k}\Big[\Big(\sigma^2\|z_i - X_k\|^2 + \mathbb{E}[E_{ij}^3]\|z_i - Z_k\| + \frac{1}{4}\mathbb{E}[E_{ij}^4] - \frac{\sigma^4}{4}\Big)(Z_k - \mu)(Z_k - \mu)^\top\Big].\end{aligned}$$

By the strong law of large numbers, we have

$$\frac{\widetilde{W}_n^\top S_B \widetilde{W}_n}{n} = \frac{1}{n}Z^\top P Z \to \Xi \in \mathbb{R}^{d\times d}$$

almost surely. Hence $(n\widetilde{W}_n^\top S_B^{-1}\widetilde{W}_n) \to \Xi^{-1}$ almost surely. Slutsky's theorem implies

$$n^{1/2}\widetilde{W}_n^\top[(\widehat{B}-B)U_B S_B^{-1/2}]_i \longrightarrow \mathcal{N}(0, \Xi^{-1}\widetilde{\Sigma}(z_i)\Xi^{-1})$$

as desired. ■

Finally we state the following lemma showing that any row of these matrices, when scaled by $n^{1/2}$, converges to 0 in probability.

Lemma 2.8.4 *For any fixed index i, we have, simultaneously*

$$n^{1/2}[(\widehat{B}-B)U_B(W^* S_{\widehat{B}}^{-1/2} - S_B^{-1/2}W^*)]_i \xrightarrow{P} 0 \tag{2.7}$$

$$n^{1/2}[U_B U_B^\top(\widehat{B}-B)U_B W^* S_{\widehat{B}}^{-1/2}]_i \xrightarrow{P} 0 \tag{2.8}$$

$$n^{1/2}[(I-U_B U_B^\top)(\widehat{B}-B)(\widehat{U}_B - U_B W^*)S_{\widehat{B}}^{-1/2}]_i \xrightarrow{P} 0 \tag{2.9}$$

$$n^{1/2}[U_B(U_B^\top U_{\widehat{B}} - W^*)S_{\widehat{B}}^{1/2}]_i \xrightarrow{P} 0. \tag{2.10}$$

$$n^{1/2}[U_B(W^* S_{\widehat{B}}^{1/2} - S_B^{1/2}W^*)]_i \xrightarrow{P} 0. \tag{2.11}$$

The rest of this section is devoted toward proving Lemma 2.8.4, for which we need the following technical lemmas controlling the spectral norm of $\|\widehat{B}-B\|$ and $\|U_B^\top \widehat{U}_B - W^*\|$ (recall that W^* is the closest orthogonal matrix, in Frobenius norm, to $U_B^\top \widehat{U}_B$.) We start with a bound for the spectral norm of $B-\widehat{B}$.

Proposition 2.8.5 $\|B-\widehat{B}\| = \mathcal{O}(\sqrt{n\log n})$ *with high probability.*

Proof: We have

$$\begin{aligned}\|B - \widehat{B}\| &= \| - \frac{1}{2}PD^2P + \frac{1}{2}P(D+E)^2P\| \\ &= \|PD \circ EP + \frac{1}{2}PE^2P\| \text{ (where } \circ \text{ is the Hadamard product)} \\ &\leq \|D \circ E\| + \frac{1}{2}\|E^2 - \mathbb{E}[E^2]\| \text{ (since } \|P\| = 1.) \\ &= \mathcal{O}(\sqrt{n}) + \mathcal{O}(\sqrt{n \log n})\end{aligned}$$

Note that here we used $\mathbb{E}[D \circ E] = 0$ and $\mathbb{E}[\frac{1}{2}PE^2P] = 0$. Each entries of $D \circ E$ is of sub-Gaussian distribution with mean 0 and each entries of $E^2 - \mathbb{E}[E^2]$ is of sub-exponential distribution with mean 0. An application of Theorem 4.4.5 in Vershynin [2018] and Matrix Bernstein for the sub-exponential case gives the desired result. ■

Lemma 2.8.6 *Let $X_1, \ldots, X_n, Y \overset{i.i.d}{\sim} F$ for some sub-Gaussian distribution F, where X_i is the ith row of the configuration matrix X of B viewed as a column vector. Let $\Xi = \mathbb{E}[X_1 {X_1}^\top]$ be of rank d, then $\lambda_i(B) = \Omega(n)$ almost surely.*

Proof: For any matrix H, the nonzero eigenvalues of $H^\top H$ are the same as those $HH^\top$, so $\lambda_i(XX^\top) = \lambda_i(X^\top X)$. In what follows, we remind the reader that X is a matrix whose rows are the transposes of the column vectors X_i, and Y is a d-dimensional vector that is independent from and has the same distribution as that of

the X_i. We observe that

$$(X^\top X - n\mathbb{E}[YY^\top])_{ij} = \sum_{k=1}^{n}(X_{ki}X_{kj} - \mathbb{E}[Y_iY_j])$$

is a sum of n independent mean-zero sub-Gaussian random variables. By a general Hoeffding's inequality for sub-gaussian random variables [Vershynin, 2018], for all $i, j \in [d]$,

$$\mathbb{P}[|(X^\top X - n\mathbb{E}[YY^\top])_{ij}| \geq t] \leq 2\exp\{\frac{-ct^2}{nM}\},$$

where $M = \max_k \|(X_{ki}X_{kj} - \mathbb{E}[Y_iY_j])\|_{\varphi_2}^2$. Therefore,

$$\mathbb{P}[|(X^\top X - n\mathbb{E}[YY^\top])_{ij}| \geq C\sqrt{n\log n}] \leq 2n^{\frac{-2C^2}{M^2}}.$$

A union bound over all $i, j \in [d]$ implies that $\|X^\top X - n\mathbb{E}[YY^\top]\|_F^2 \leq C^2d^2n\log n$ with probability at least $1 - 2n^{-2C^2/M^2}$, i.e. $\|X^\top X - n\mathbb{E}[YY^\top]\|_F \leq Cd\sqrt{n\log n}$ with high probability for any $C > \frac{M}{\sqrt{2}}$. By the Hoffman-Wielandt inequality, $|\lambda_i(XX^\top) - n\lambda_i(\mathbb{E}[YY^\top])| \leq Cd\sqrt{n\log n}$, and by reverse triangle inequality, we obtain

$$\lambda_i(XX^\top) \geq \lambda_d(XX^\top) \geq |n\lambda_d(\Xi)| - Cd\sqrt{n\log n} = \Omega(n)$$

holds almost surely. ■

Proposition 2.8.7 *Let $W_1\Sigma{W_2}^T$ be the singular value decomposition of $U_B^\top U_{\widehat{B}}$, then*

with high probability, $\|U_B^\top U_{\widehat{B}} - W_1 W_2{}^\top\| = \mathcal{O}(n^{-1}\log n)$.

Proof: Let $\sigma_1, \sigma_2, \ldots, \sigma_d$ be the singular values of $U_B^\top U_{\widehat{B}}$ (the diagonal entries of Σ). Then $\sigma_i = \cos(\theta_i)$ where θ_i's are the principal angles between the subspace spanned by U_B and $U_{\widehat{B}}$. The Davis-Kahan $\sin(\Theta)$ theorem [Davis and Kahan, 1970] gives

$$\|U_{\widehat{B}} U_{\widehat{B}}^\top - U_B U_B^\top\| = \max_i |\sin(\theta_i)| \leq \frac{C\|B - \widehat{B}\|}{\lambda_d(B)} = \mathcal{O}(\sqrt{\frac{\log n}{n}})$$

for sufficiently large n. Note in the last equality we used the previous two lemmas. Thus,

$$\begin{aligned} ||U_B^\top U_{\widehat{B}} - W_1 W_2{}^\top||_F = ||\Sigma - I||_F &= \sqrt{\sum_{i=1}^{d}(1-\sigma_i)^2} \leq \sum_{i=1}^{d}(1-\sigma_i) \leq \sum_{i=1}^{d}(1-{\sigma_i}^2) \\ &= \sum_{i=1}^{d}\sin(\theta_i)^2 \leq d||U_{\widehat{B}} U_{\widehat{B}}^\top - U_B U_B^\top||^2 = \mathcal{O}(\frac{\log n}{n}) \end{aligned}$$

■

Recall that a random vector X is sub-exponential if $\mathbb{P}[|X| > t] \leq 2e^{-\frac{t}{K}}$ for some constant K and for all $t \geq 0$. Associated with a sub-exponential random variable there is a Orlicz norm defined as $\|X\|_{\psi_1} = \inf\{t > 0 : \mathbb{E}\exp(\frac{|X|}{t}) \leq 2\}$. Furthermore, a random variable X is sub-Gaussian if and only if X^2 is sub-exponential, and $\|X^2\|_{\psi_1} = \|X\|_{\psi_2}^2$. We now have the following lemma which allows us to juxtapose the ordering in the matrix product $W^*\widehat{S}_B$ and $S_B W^*$ (and similarly $W^*\widehat{S}_B^{1/2}$ and $S_B^{1/2}W^*$.) This juxtaposition is essential in showing Eq. (2.7) and Eq. (2.11) in Lemma 2.8.4.

Lemma 2.8.8 *Let $W^* = W_1 W_2{}^\top$. Then with high probability,*

$$\|W^* S_{\widehat{B}} - S_B W^*\|_F = \mathcal{O}(\log n); \quad \textit{and} \quad \|W^* S_{\widehat{B}}^{1/2} - S_B^{1/2} W^*\|_F = \mathcal{O}(n^{-\frac{1}{2}} \log n).$$

Proof: Let $R = U_{\widehat{B}} - U_B U_B^\top U_{\widehat{B}}$. Note R is the residual after projecting $U_{\widehat{B}}$ orthogonally onto the column space of U_B, and thus $\|U_{\widehat{B}} - U_B U_B^\top U_{\widehat{B}}\|_F \leq \min_W \|U_{\widehat{B}} - U_B W\|_F$ where the minimization is over all orthogonal matrices W. By a variant of the Davis-Kahan $\sin\Theta$ theorem [Yu et al., 2015], we have

$$\min_W \|U_B W - U_{\widehat{B}}\|_F \leq \frac{C\sqrt{d}\|B - \widehat{B}\|}{\lambda_d(B)},$$

and hence $\|R\|_F \leq \mathcal{O}(\sqrt{\frac{\log n}{n}})$. Now consider

$$\begin{aligned}
W^* S_{\widehat{B}} &= (W^* - U_B^\top U_{\widehat{B}}) S_{\widehat{B}} + U_B^\top U_{\widehat{B}} S_{\widehat{B}} \\
&= (W^* - U_B^\top U_{\widehat{B}}) S_{\widehat{B}} + U_B^\top \widehat{B} U_{\widehat{B}} \\
&= (W^* - U_B^\top U_{\widehat{B}}) S_{\widehat{B}} + U_B^\top (\widehat{B} - B) U_{\widehat{B}} + U_B^\top B U_{\widehat{B}} \\
&= (W^* - U_B^\top U_{\widehat{B}}) S_{\widehat{B}} + U_B^\top (\widehat{B} - B) R + U_B^\top (\widehat{B} - B) U_B U_B^\top U_{\widehat{B}} + S_B U_B^\top U_{\widehat{B}}.
\end{aligned}$$

Note here we use the fact $U_{\widehat{B}} S_{\widehat{B}} = \widehat{B} U_{\widehat{B}}$. Now write

$$S_B U_B^\top U_{\widehat{B}} = S_B (U_B^\top U_{\widehat{B}} - W^*) + S_B W^*,$$

then we have

$$W^*S_{\widehat{B}} - S_B W^* = (W^* - U_B^\top U_{\widehat{B}})S_{\widehat{B}} + U_B^\top(\widehat{B} - B)R + U_B^\top(\widehat{B} - B)U_B U_B^\top U_{\widehat{B}} + S_B(U_B^\top U_{\widehat{B}} - W^*).$$

This gives

$$\begin{aligned}
\|W^*S_{\widehat{B}} - S_B W^*\|_F \leq\ & \|(U_B^\top U_{\widehat{B}} - W^*)(S_{\widehat{B}} + S_B)\|_F + \|U_B^\top(\widehat{B} - B)R\|_F \\
& + \|U_B^\top(\widehat{B} - B)U_B U_B^\top U_{\widehat{B}}\|_F \\
\leq\ & \|(U_B^\top U_{\widehat{B}} - W^*)\|_F(\|S_{\widehat{B}}\| + \|S_B\|) + \|U_B^\top(\widehat{B} - B)R\|_F \\
& + \|U_B^\top(\widehat{B} - B)U_B U_B^\top U_{\widehat{B}}\|_F \\
\leq\ & \|W_1 W_2^\top - U_B^\top U_{\widehat{B}}\|_F(\mathcal{O}(n) + \mathcal{O}(n)) + \|U_B^\top(\widehat{B} - B)R\|_F \\
& + \|U_B^\top(\widehat{B} - B)U_B\|_F \\
\leq\ & \mathcal{O}(n^{-1})(\mathcal{O}(n) + \mathcal{O}(n)) + \mathcal{O}(\log n) + \|U_B^\top(\widehat{B} - B)U_B\|_F \\
=\ & \mathcal{O}(\log n) + \|U_B^\top(\widehat{B} - B)U_B\|_F.
\end{aligned}$$

Now consider the term $U_B^\top(\widehat{B} - B)U_B \in \mathbb{R}^{d\times d}$. If we denote U_i be the ith column of U_B, then for each i, jth entry, we have

$$(U_B^\top(\widehat{B} - B)U_B)_{ij} = U_i^\top(\widehat{B} - B)U_j = \frac{1}{2}V_i^\top(\Delta^2 - D^2)V_j$$

where $V = PU_B$. Furthermore, we have

$$V_i^\top(\Delta^2 - D^2)V_j = \sum_{k,l} V_{ik}({\Delta_{kl}}^2 - {D_{kl}}^2)V_{jl}. \tag{2.12}$$

Recall, since X_k's are sub-Gaussian, thus equation (2.12) is a sum of mean zero sub-exponential random variables. By Bernstein's inequality [Vershynin, 2018], we have

$$\mathbb{P}[|\sum_{k,l}({\Delta_{kl}}^2 - {D_{kl}}^2)V_{ik}V_{jl}| > t] \leq 2\exp\Big\{-C\min(\frac{t^2}{M^2\sum_{k,l}{V_{ik}}^2{V_{kl}}^2}, \frac{t}{M\max_{k,l}(V_{ik}V_{jl})})\Big\}$$

where $M := \max_{k,l}\|{\Delta_{kl}}^2 - {D_{kl}}^2\|_{\psi_1}$. Since $\sum_k {V_{ik}}^2 \leq 1 \forall i$, we have that each entry of $U_B^\top(\widehat{B} - B)U_B \in \mathbb{R}^{d\times d}$ is $\mathcal{O}(\log n)$, and

$$\|U_B^\top(\widehat{B} - B)U_B\|_F = \mathcal{O}(\log n). \tag{2.13}$$

This then gives $\|W^* S_{\widehat{B}} - S_B W^*\|_F = \mathcal{O}(\log n)$, with high probability.

Finally, consider $\|W^* S_{\widehat{B}}^{1/2} - S_B^{1/2} W^*\|_F$. The i,jth entry of $W^* S_{\widehat{B}}^{1/2} - S_B^{1/2} W^*$ is

$$\begin{aligned} {W^*}_{ij}({\lambda_j}^{1/2}(\widehat{B}) - {\lambda_i}^{1/2}(B)) =& {W^*}_{ij}\frac{\lambda_j(\widehat{B}) - \lambda_i(B)}{{\lambda_j}^{1/2}(\widehat{B}) + {\lambda_i}^{1/2}(B)} \leq {W^*}_{ij}\frac{\lambda_j(\widehat{B}) - \lambda_i(B)}{\Omega(\sqrt{n})} \\ =& \mathcal{O}(n^{-\frac{1}{2}}\log n), \end{aligned}$$

as desired (note in the last inequality, we used the first part of this Lemma. ■ We now proceed to prove Lemma 2.8.4.

Proof: [Proof of Lemma 2.8.4]

To show Eq. (2.7), we have

$$\begin{aligned}\sqrt{n}\|(\widehat{B}-B)U_B(W^*S_{\widehat{B}}^{-1/2}-S_B^{-1/2}W^*)\|_F &\leq \sqrt{n}\|(\widehat{B}-B)U_B\| \times \|W^*S_{\widehat{B}}^{-1/2}-S_B^{-1/2}W^*\|_F \\ &\leq \sqrt{n}\|(\widehat{B}-B)\| \times \|W^*S_{\widehat{B}}^{-1/2}-S_B^{-1/2}W^*\|_F \\ &= \sqrt{n}\mathcal{O}(\sqrt{n\log n})\mathcal{O}(n^{-\frac{3}{2}}\log n) = \frac{C\log n\sqrt{\log n}}{\sqrt{n}}\end{aligned}$$

which converges to 0 as $n \to \infty$.

Let us now consider Eq. (2.8). Recall that $X = U_B S_B^{1/2} W$ for some orthogonal matrix W, and since X_i's are sub-Gaussian, $\|X_i\|$ is bounded by some constant C with high probability, i.e., $\|X_i\| = \sqrt{\sum_{j=1}^{d} \sigma_j {U_B}_{ij}^2} \leq C$ with high probability, where σ_i's are the diagonal entries of $S_B^{1/2}$. Note that $\sigma_i = \Omega(n) \geq C'n$ for all i and some constant C'. We thus obtain $\sqrt{\sum_{j=1}^{d} {U_B}_{ij}^2} \leq \frac{C}{\sqrt{n}}$, i.e., $||U_B||_{2\to\infty} \leq \frac{C}{\sqrt{n}}$. Hence,

$$\begin{aligned}\|[U_B U_B^\top(\widehat{B}-B)U_B W^* S_{\widehat{B}}^{-1/2}]_h\| &\leq \|U_B\|_{2\to\infty}\|U_B^\top(\widehat{B}-B)U_B\| \times \|S_{\widehat{B}}^{-1/2}\| \\ &\leq \frac{C}{\sqrt{n}}\mathcal{O}(\log n)\mathcal{O}(n^{-\frac{1}{2}}) \leq \frac{C\log n}{n}\end{aligned}$$

which also converges to 0 as $n \to \infty$ (note in the last inequality we used 2.13).

To show Eq. (2.9), we must bound $\|[(I - U_B U_B^\top)(\widehat{B}-B)(\widehat{U}_B - U_B W^*)S_{\widehat{B}}^{-1/2}]_h\|$.

Define

$$G_1 = (I - U_B U_B^\top)(\widehat{B} - B)(I - U_B U_B^\top)U_{\widehat{B}} S_{\widehat{B}}^{-1/2},$$
$$G_2 = (I - U_B U_B^\top)(\widehat{B} - B)U_B(U_B^\top U_{\widehat{B}} - W^*)S_{\widehat{B}}^{-1/2}$$

Note that $(I - U_B U_B^\top)(\widehat{B} - B)(\widehat{U}_B - U_B W^*){S_{\widehat{B}}}^{-1/2} = G_1 + G_2$. We now only need to bound the hth row of G_1 and G_2.

$$\begin{aligned}
\|G_2\|_F &\leq \|(I - U_B U_B^\top)(\widehat{B} - B)U_B\| \times \|U_B^\top U_{\widehat{B}} - W^*\|_F \times \|{S_{\widehat{B}}}^{-\frac{1}{2}}\| \\
&\leq \|(I - U_B U_B^\top)\| \times \|\widehat{B} - B\| \times \|U_B^\top U_{\widehat{B}} - W^*\|_F \times \|{S_{\widehat{B}}}^{-\frac{1}{2}}\| \\
&= \mathcal{O}(1)\mathcal{O}(\sqrt{n \log n})\mathcal{O}(n^{-1})\mathcal{O}(n^{-\frac{1}{2}}) = \mathcal{O}(\frac{\sqrt{\log n}}{n})
\end{aligned}$$

Thus $\|\sqrt{n}G_2\|_F$ converges to 0 as $n \to \infty$. We now consider the rows of G_1. Note that $U_{\widehat{B}}^\top U_{\widehat{B}} = I$ and hence

$$\begin{aligned}
\|(G_1)_h\| &= \|[(I - U_B U_B^\top)(\widehat{B} - B)(I - U_B U_B^\top)U_{\widehat{B}} S_{\widehat{B}}^{-1/2}]_h\| \\
&= \|[(I - U_B U_B^\top)(\widehat{B} - B)(I - U_B U_B^\top)U_{\widehat{B}} U_{\widehat{B}}^\top U_{\widehat{B}} S_{\widehat{B}}^{-1/2}]_h\| \\
&= \|U_{\widehat{B}} S_{\widehat{B}}^{-1/2}\| \times \|[(I - U_B U_B^\top)(\widehat{B} - B)(I - U_B U_B^\top)U_{\widehat{B}} U_{\widehat{B}}^\top]_h\| \\
&\leq \frac{C}{\sqrt{n}}\|[(I - U_B U_B^\top)(\widehat{B} - B)(I - U_B U_B^\top)U_{\widehat{B}} U_{\widehat{B}}^\top]_h\|
\end{aligned}$$

Define

$$H_1 = (I - U_B U_B^\top)(\widehat{B} - B)(I - U_B U_B^\top)U_{\widehat{B}} U_{\widehat{B}}^\top.$$

Since the Z_i are i.i.d., the rows of H_1 are exchangeable and hence, for any fixed index h, $n\mathbb{E}\|(H_1)_h\|^2 = \mathbb{E}[\|H_1\|_F^2]$. Markov's inequality then implies

$$\begin{aligned}\mathbb{P}[\|\sqrt{n}(H_1)_h\| > t] &\leq \frac{n\mathbb{E}\|[(I - U_B U_B^\top)(\widehat{B} - B)(I - U_B U_B^\top)U_{\widehat{B}} U_{\widehat{B}}^\top)_h]\|^2}{t^2} \\ &= \frac{\mathbb{E}\big(\|(I - U_B U_B^\top)(\widehat{B} - B)(I - U_B U_B^\top)U_{\widehat{B}} U_{\widehat{B}}^\top\|_F^2\big)}{t^2}\end{aligned}$$

Furthermore,

$$\|(I - U_B U_B^\top)(\widehat{B} - B)(I - U_B U_B^\top)U_{\widehat{B}} U_{\widehat{B}}^\top\|_F \leq \|\widehat{B} - B\| \times \|U_{\widehat{B}} - U_B U_B^\top U_{\widehat{B}}\|_F$$

We now recall the following two observations

- The optimization problem $\min_{T \in \mathbb{R}^{d\times d}} \|U_{\widehat{B}} - U_B T\|_F^2$ is solved by $T = U_B^\top U_{\widehat{B}}$.
- By theorem 2 of Yu et al. [2015], there exists $W \in \mathbb{R}^{d\times d}$ orthogonal, such that $\|U_{\widehat{B}} - U_B W\|_F \leq C\|U_{\widehat{B}} U_{\widehat{B}}^\top - U_B U_B^\top\|_F$.

Combining the two facts above, we conclude that $\|U_{\widehat{B}} - U_B U_B^\top U_{\widehat{B}}\|_F^2 \leq \frac{C}{n}$ with high probability, as in Lemma 2.8.8, hence

$$\|(I - U_B U_B^\top)(\widehat{B} - B)(I - U_B U_B^\top)U_{\widehat{B}} U_{\widehat{B}}^\top\|_F \leq \mathcal{O}(\sqrt{n \log n})\frac{C}{\sqrt{n}} = \mathcal{O}(\sqrt{\log n}),$$

with high probability. Therefore,

$$\mathbb{P}(\|\sqrt{n}(H_1)_h\| > t) \leq \frac{\sqrt{\log n}}{t^2}.$$

picking $t = n^{\frac{1}{4}}$, we get $\lim_{n\to\infty} Cn^{-1/2}\|\sqrt{n}(H_1)_h\| = 0$.

Finally, Eq. (2.10) and Eq. (2.11) follow from Lemma 2.8.7 and Lemma 2.8.8 and the bound $\|U_B\|_{2\to\infty} \leq Cn^{-1/2}$. ■

2.8.2 Adaptation for Theorem 2.4.1 and 2.4.4

The major difference between our main theorems is the calculation of the covariance matrices. In this section, we will give those calculations.

Lemma 2.8.9 *Let $Z_1, \ldots, Z_n$ be independent and identically distributed according to some multivariate sub-Gaussian distribution F and let our model be as in Theorem 2.4.1. Then there exists a sequence of $d \times d$ orthogonal matrices $\widetilde{W}_n$, such that for any fixed index i, we have*

$$n^{1/2}\widetilde{W}_n^\top[(\widehat{B} - B)U_B S_B^{-1/2}]_i \longrightarrow \mathcal{N}(0, \Sigma)$$

where $\Sigma = \frac{\sigma^2}{4}\Xi^{-1}$, $\Xi = \mathrm{cov}(Z_k)$. Here $(A)_i$ or $[A]_i$ denote the ith row of a matrix A.

Proof: Recall that $PZ = U_B S_B^{1/2} \widetilde{W}_n$. We therefore have

$$
\begin{aligned}
n^{1/2}\widetilde{W}_n^\top[(\widehat{B}-B)U_B S_B^{-1/2}]_i &= n^{1/2}\widetilde{W}_n^\top[(\widehat{B}-B)PZ\widetilde{W}_n^\top {S_B}^{-1}]_i \\
&= n^{1/2}\widetilde{W}_n^\top {S_B}^{-1}\widetilde{W}_n[(\widehat{B}-B)PZ]_i \\
&= \frac{1}{2}n^{1/2}\widetilde{W}_n^\top {S_B}^{-1}\widetilde{W}_n[P(D^{(2)}-\Delta^{(2)})PZ]_i \\
&= \frac{1}{2}n^{1/2}\widetilde{W}_n^\top {S_B}^{-1}\widetilde{W}_n\Big[P(D^{(2)}-\Delta^{(2)})(I-1_n 1_n^\top/n)Z\Big]_i \\
&= \frac{1}{2}n^{1/2}\widetilde{W}_n^\top {S_B}^{-1}\widetilde{W}_n\Big[P(D^{(2)}-\Delta^{(2)})(Z-1_n\mu^\top)\Big]_i \\
&\quad (\text{ since } PZ = Z - 1_n\bar{Z} = Z - 1_n\mu^\top) \\
&= \frac{1}{2}n^{1/2}\widetilde{W}_n^\top {S_B}^{-1}\widetilde{W}_n\Big[(D^{(2)}-\Delta^{(2)})(Z-1_n\mu^\top) \\
&\quad - 1_n 1_n^\top/n(D^{(2)}-\Delta^{(2)})(Z-1_n\mu^\top)\Big]_i \\
&\quad (\text{note that } \frac{1_n 1_n^\top}{n}(D^{(2)}-\Delta^{(2)})(Z-1_n\mu^\top) \to 0 \text{ as } n\to\infty) \\
&= \frac{1}{2}n^{1/2}\widetilde{W}_n^\top {S_B}^{-1}\widetilde{W}_n\Big[(D^{(2)}-\Delta^{(2)})(Z-1_n\mu^\top)\Big]_i \text{ as } n\to\infty
\end{aligned}
$$

Therefore,

$$
n^{1/2}\widetilde{W}_n^\top[(\widehat{B}-B)U_B S_B^{-1/2}]_i = \frac{1}{2}n\widetilde{W}_n^\top S_B^{-1}\widetilde{W}_n\Big[n^{-1/2}\sum_{j\neq i}^{n}\Big(D_{ij}^{(2)}-\Delta_{ij}^{(2)}\Big)(Z_j-\mu)\Big]
$$

Conditioning on $Z_i = z_i$, the above expression is sum of $n-1$ independent mean 0 random vectors. We then invoke the Lindeberg-Feller central limit theorem to show that this sum converges to a multivariate normal. We now evaluate the covariance

matrix for this sum. Each summand has covariance matrix of the form

$$\begin{aligned}\operatorname{cov}\Big[(D_{ij}^{(2)} - \Delta_{ij}^{(2)})(Z_j - \mu)\Big] &= \operatorname{Var}\Big(D_{ij}^{(2)} - \Delta_{ij}^{(2)}\Big)(Z_j - \mu)(Z_j - \mu)^\top \\ &= \sigma^2 (Z_j - \mu)(Z_j - \mu)^\top \\ &\text{Since } \mathbb{E}[E_{ij}] = 0 \text{ and } \mathbb{E}[E_{ij}^2] = \sigma^2\end{aligned}$$

. By the strong law of large numbers, we have

$$\frac{\widetilde{W}_n^\top S_B \widetilde{W}_n}{n} = \frac{1}{n} Z^\top P Z \to \Xi \in \mathbb{R}^{d \times d}$$

almost surely. Hence $(n\widetilde{W}_n^\top S_B^{-1} \widetilde{W}_n) \to \Xi^{-1}$ almost surely. Slutsky's theorem implies

$$n^{1/2} \widetilde{W}_n^\top [(\widehat{B} - B) U_B S_B^{-1/2}]_i \longrightarrow \mathcal{N}(0, \frac{\sigma^2}{4} \Xi^{-1})$$

as desired. ■

Lemma 2.8.10

Chapter 3

Manifold Denoising with Unsupervised Randomer Forest

3.1 Introduction

The accuracy, scalability, and applicability of many machine learning algorithms is currently impeded by the high-dimensional and large-scale nature of most modern data sets. In particular, the dimensionality, or number of features, of many data sets is often high, often due to noise in the data – each data point is represented as a high-dimensional vector, but only a subset of them actually carries signals for subsequent inference. In other words, the data may lives near some unknown low-dimensional manifold embedded in some high-dimensional space. To gain a thorough understanding of the data, it is therefore often necessary to reduce its dimensionality

in a way that preserves its underlying structure. *Manifold learning* is a set of tools designed to recover the underlying latent low-dimensional manifold structures of high-dimensional data.

Existing manifold learning methods, however, face a number of challenges. Linear approaches such as principal component analysis (PCA) Pearson [1901], independent component analysis (ICA) Hyvärinen and Oja [2000], canonical correlation analysis (CCA) Hotelling [1936], multidimensional scaling (MDS)Cox and Cox [2000], CUR decompositions Mahoney and Drineas [2009], and Fisher's linear discriminant analysis (LDA), have been widely applied and useful in many domains, but make fairly strong assumptions of about a linear structure underlying a data set. To mitigate these issues a number of methods that can be characterized as kernel PCA methods were devised Schölkopf et al. [1997], including Isomap Tenenbaum et al. [2000b], Laplacian eigenmaps Belkin and Niyogi [2002], maximum variance unfolding Weinberger and Saul [2006]. These approaches are quite fragile to algorithm parameters, and typically require $mathcal{O}(n^3)$ operations for n samples, which is prohibitively computationally expensive for many datasets. Methods based on exact nearest neighbors, such as t-Distributed Stochastic Neighbor Embedding (t-SNE) Maaten and Hinton [2008], and Uniform Manifold Approximation and Projection (UMAP) McInnes and Healy [2018] also suffer computationally for large n. Approximate nearest neighbor approaches can mitigate some of these computational issues. For example, Fast Approximate Nearest-Neighbor Matching (FLANN) Muja and Lowe [2014] is a popular

algorithm for nearest-neighbor detection in high-dimensional data sets. But FLANN, like all the above mentioned manifold learning algorithms, always operates on the observed dimensionality of the data. When the true manifold is low-dimensional, and the data are high-dimensional, the additional noise dimensions will be problematic for any of these algorithms.

We there propose an approach that we dub *Unsupervised Randomer Forest* (URerF). Unlike the previously described methods, URerF does not need to compute geodesic distances between pairs of points. Instead, URerF examines local structure by recursively clustering data in a sparse linear subspace of the original data, building on the recently proposed randomer forest algorithm for supervised learning Tomita et al. [2015]. This randomer forest approach allows URerF to separate meaningful structure in the data from the noise dimensions.

Another contribution of this manuscript is a novel method for evaluating manifold learning algorithms. Most existing manuscripts on the topic either embed the data into some low-dimensional space, such as 2D or 3D, and then merely visualize the results. This approach is obviously limited in a number of ways: (1) it is purely qualitative, (2) when the structure is higher dimensional it may be lost, and (3) it relies on an embedding, which introduces additional complications. Other manuscripts compare the results on some subsequent inference task, such as classification. Such an approach is only able to evaluate performance of the manifold learning algorithm composed with a particular subsequent inferential method, but not the

manifold learning algorithm itself. We therefore introduce Precision@K, Recall@K, and Precision-Recall curves as quantitative metrics to evaluate manifold learning. The difference between our proposed metrics and standard metrics, is that we do not evalute nearest neighbors with respect to the high-dimensional observed data, but rather the true low-dimensional latent representations. If a manifold learning does poorly on this metric, it has no hope to perform well on subsequent tasks. Indeed Precision@k provides a theoretical bound on subsequent classification accuracy Devroye et al. [1997].

3.2 Related Work

Of the many previously proposed manifold learning algorithms, we describe a few in detail that have risen to prominence and widespread use, which we will later compare to URerF.

One of the most widely used methods for nonlinear dimensionality reduction is still Isomap Tenenbaum et al. [2000b], which constructs a low-dimensional embedding of input data by first finding geodesic distances between data points in a k-nearest neighbor graph, then applies classical multidimensional scaling to the matrix of graph distances. In the case of many noisy dimensions, however, the Isomap algorithm can fail to construct an accurate nearest-neighbor graph, and requires the storage of all point-to-point graph distances, which incurs both a large space and time complexity.

UMAP is a new algorithm for dimensionality reduction that efficiently reduces high-dimensional data to a low dimension using a fuzzy simplicial set representation of the input data points McInnes and Healy [2018]. Like other nearest-neighbor based algorithms, UMAP first constructs an undirected, weighted k-nearest neighbor graph from the input data, then embeds data points in a low-dimensional space using a force directed layout algorithm. The number of neighbors used to construct the graph in effect determines the local manifold structure that is to be preserved in the low-dimensional layout. In the force-directed layout approach, attractive forces between close vertices are iteratively balanced with repulsive forces between vertices that are far apart in the graph until convergence. UMAP builds upon the popular t-Distributed Stochastic Neighbor Embedding (t-SNE) algorithm, which attempts to preserve original interpoint distances in a much lower dimensional space. The Kullback-Leibler between the distribution of neighbor distances in the higher and lower dimensional spaces is used to determine the optimal mapping of points into the lower-dimensional space. t-SNE is primarily used for the visualization of high-dimensional data Maaten and Hinton [2008], and cannot be used with non-metric distances. The UMAP algorithm was shown to produce similar embeddings to t-SNE in two or three dimensions, but to scale better in terms of runtime across a wide range of embedding dimensions McInnes and Healy [2018].

Finally, most closely related to our method are existing unsupervised random forest methods, the most popular of which is included in Adele Cutler's RandomForest

R package Shi and Horvath [2006]. It proceeds by generating a synthetic copy of the data by randomly permuting each feature independently of the others, and then attempts to classify the real versus the synthetic dataset. As will be seen below, this approach leads to missing surprisingly easy latent structures.

3.3 Unsupervised Randomer Forests

Our unsupervised random forest algorithm is based on the original Random Forest algorithm invented by Breiman Breiman [2001] with a few key distinctions. A random forest is an ensemble of decision trees where each tree is created from bootstrapped samples of the training dataset in order to incorporate randomness. That is, each tree is built from a random subset of training data. More formally, a random forest is as a classifier consisting of a collection of tree structured classifiers $\{h(\mathbf{x}, \theta_k)\}, k = 1, 2..$ numtrees where θ_k's are parameters and each tree casts a unit vote for the most popular class at input $\mathbf{x}$.

Random Forests can be used for both supervised and unsupervised situations. In particular, for the unsupervised case, we can build a similarity matrix from the random forest. The similarity between two data points X_1 and X_2 is estimated as the fraction of the trees in which X_1 and X_2 appear in the same leaf node.

Our method additionally differs from the traditional, supervised case in the following ways. First, we describe three different splitting criteria to rank potential

splits, inspired by techniques studied in clustering research. We also show empirically that a novel FastBIC split results in better precision and recall accuracy because we incorporate model selection at each node. In past literature, these splitting criteria have not been explored in conjunction with decision trees and random forests.

Second, we use the term *randomer* to label our technique, as our splitting methods are in addition based on random sparse linear combination of features to further improve randomness, as in Tomita et al.'s *Randomer Forests* algorithm Tomita et al. [2015]. Randomness is therefore incorporated into the forest generation process in candidate dimension generation stage as well as the traditionally randomness-inducing bagging stage.

Third, we correctly implement a previously proposed method for generating proximity matrices from random forests. Specifically, in the currently most widely used implementation of Random Forest Liaw and Wiener [2002], the aggregated normalized proximity matrices of N Random Forests with M trees each is not stochastically equivalent to the aggregated normalized proximity matrices of M Random Forests with N trees each. We fix this bug in our implementation.

3.4 Algorithm

3.4.1 Overall algorithm

Given an input data set $X = \{x_1, \ldots, x_n\}$, T decision trees are built, each from a random sample of size $m < n$. In each tree, URerF recursively splits a parent node into its two child nodes. Each internal node bisects the data based on its value in a particular dimension or on its values in a linear combination of a small number of dimensions. The best dimension, or combination of dimensions, is selected to split on based on the score that results from the splitting criteria described in Section 3.4.2. The proximity matrix is then populated by computing the fraction of the trees in which every pair of elements reside in the same leaf node. Algorithm 1 describes the algorithm to build the forest and Algorithm 2 describes the tree building process. Algorithms 3 - 5 describe the splitting procedures. All algorithms are relegate to Section 3.5.

3.4.2 Splitting Criteria

We have implemented and compared several splitting criteria in our evaluation of the unsupervised randomer forest algorithm. Namely, we compare splitting by 2-means clustering, two-means clustering with the Bayesian Information Criterion (BIC) test, and a soft clustering as defined by the most likely Gaussian Mixture

Model (GMM) of two Gaussians with the BIC test. The advantage of incorporating the BIC test into our splitting mechanism is its ability to select the the split which results in two distinct clusters. The BIC test outputs a score which is a measure of how well the datapoints are explained by a Gaussian mixture model with two Gaussians.

3.4.2.1 Two-Means Splitting

We aim to find the split which minimizes the sum of the intra-cluster variance on the projected dimension. The elements are first sorted. Each element is scanned to be a potential cut point. The element to the left form one cluster with mean μ_1 and the elements to the right of the cutpoint form another cluster with mean μ_2. We seek to find the cutpoint which minimizes the one-dimensional 2-means objective

$$\sum_{i=1}^{N_1}(X_i - \mu_1)^2 + \sum_{i=N_1}^{N_1+N_2}(X_i - \mu_2)^2.$$

The algorithmic details are explained in Algorithm 3.

3.4.2.2 Two-Means Splitting with FastBIC

The Bayesian Information Criterion (BIC) is used to select from among a finite collection of models. It is based on the log likelihood of the model given the points, with a regularization term penalizing complex models with many parameters. Con-

cretely, the BIC score (y) can be defined as follows.

$$y = \ln(n)d - 2\ln(\widehat{L}) \tag{3.1}$$

Here $\widehat{L}$ is the maximum log likelihood function of a particular model M, n is the sample size (number of data points) and d is the number of parameters estimated by the model. The maximum likelihood is defined as $\widehat{L} = p(x|\widehat{\theta}, M)$, where $\widehat{\theta}$ are the parameters that maximize the likelihood function, and x is the observed data, for the model M.

We rank potential splits on the BIC score obtained assuming a model with a mixture of two Gaussians; the sorted elements along a given dimension to the left of the cut point belong to one Gaussian and the elements to the right belong to another Gaussian. Note here, that this is slightly different from a Gaussian mixture model because here we assume the that the point has been generated from each Gaussian k with a fixed (known) probability π_k which is the fraction of data points on either end of the split.

For example, if the elements in one dimension are $\{1, 3, 4, 6\}$, then the possible splits are $\{\{1\}, \{3, 4, 6\}\}$, $\{\{1, 3\}, \{4, 6\}\}$, and $\{\{1, 3, 4\}, \{6\}\}$. In the case $\{\{1, 3\}, \{4, 6\}\}$, we assume the model to comprise of two univariate Gaussians where $\{1, 3\}$ are sampled from the first and $\{4, 6\}$ are sampled from the second. $\pi_1 = \pi_2 = 0.5$ in this case, as an equal number of points are sampled from both Gaussians. We compute

the estimates μ_1, μ_2 and σ_1^2, σ_2^2 for the means and variances of each of the two Gaussians in order to find the likelihood of the data under this split, and use it to compute the BIC score. The BIC score is computed for each possible split and we assign this dimension to the split which results in the lowest BIC score. We proceed in the same manner for all dimensions and choose to split using the dimension which results in the lowest overall BIC score. The model can be defined as follows. $P(x_1, .., x_n|\mu, \sigma, \pi)$ is defined as follows, where $\mu = (\mu_1, ..., \mu_K)$, $\sigma = (\sigma_1, ..., \sigma_K)$, $\pi = (\pi_1, ..., \pi_K)$:

$$P(x_{1:N}, z_{1:N,1:K}|\mu_{1:K}, \sigma, \pi) = \prod_{n=1}^{N}\prod_{k=1}^{K}\{\pi_k \mathcal{N}(x_n|\mu_k, \sigma_k^2)\}^{z_{n,k}} \tag{3.2}$$

Here N is the number of observations and K is the number of Gaussian clusters. In this case $K = 2$. We assume the points to the left of the split point form one cluster and the points to right form the second cluster. $z_i \in \{0, 1\}^K$ is the indicator vector for data point x_i: $z_{(i\in(0,s],k=0)} = 1$ and $z_{(i\in[s+1,N),k=1)} = 1$ and 0 otherwise. Now, letting the split point be x_s, $x_1..x_s$ belong to cluster 1 and $x_{s+1}..x_n$ belong to cluster 2. The likelihood can be obtained by summing over the zs as follows.

$$P(x|\mu, \sigma, \pi) = \sum_{z_{1:N,1:K}} \prod_{n=1}^{N}\prod_{k=1}^{K}\{\pi_k \mathcal{N}(x_n|\mu_k, \sigma_k^2)\}^{z_{n,k}} \tag{3.3}$$

Equation (3.3) can be simplified by noting that $z_{(i\in(0,s],k=0)} = 1$ and $z_{(i\in[s+1,N),k=1)} =$

1 and 0 otherwise.

$$P(x|\mu,\sigma,\pi) = \prod_{n=1}^{s} \pi_1 \mathcal{N}(x_n|\mu_1,\sigma_1^2) \prod_{n=s+1}^{N} \pi_2 \mathcal{N}(x_n|\mu_2,\sigma_2^2) \tag{3.4}$$

The maximum log likelihood function

$\widehat{L} = \log P(x_1, x_2, ..., x_N|\widehat{\mu}_{1:K}, \widehat{\sigma}_{1:k}, \widehat{\pi}_{1:k})$ is given by

$$\widehat{L} = \sum_{n=1}^{s} [\log \pi_1 + \log \mathcal{N}(x_n|\widehat{\mu_1}, \widehat{\sigma_1}^2)] + \sum_{n=s+1}^{N} [\log \pi_2 + \log \mathcal{N}(x_n|\widehat{\mu_2}, \widehat{\sigma_2}^2)] \tag{3.5}$$

Here, $\widehat{\sigma}_k$ and $\widehat{\mu}_k$ are the estimates of σ_k and μ_k which maximize the log likelihood function. Let $N_1 = s$ and $N_2 = N - (s+1)$. Then, $\mu_k = \frac{1}{N_k}\sum_{n=1}^{N_k} x_n$, $\widehat{\sigma_k} = \frac{1}{N_k}\sum_{n=1}^{N_k} ||x_n - \widehat{\mu_k}||^2$, and $\widehat{\pi}_k = \frac{N_k}{N}$. We further test for the single variance case ($\sigma_1 = \sigma_2$) and use the BIC formula to determine the best case. Substituting into equation 3.5 and simplifying, we get the following expression for the log likelihood.

$$\widehat{L} = -\frac{N_1}{2} \log 2\widehat{\pi}\widehat{\sigma}_1^2 - \frac{N_2}{2} \log 2\widehat{\pi}\widehat{\sigma}_2^2, \tag{3.6}$$

where we have dropped a number of terms that are not functions of the parameters. This FastBIC procedure is, to our knowledge, novel.

3.4.2.3 2-GMM Splitting with BIC

The GMM likelihood equations are the same as in the above case, except we now relax the binary constraints on the z_i. Specifically, each point is considered to belong to weighted sum of the two Gaussians as opposed to a single Gaussian. We do not know the values of z_i and we iteratively estimate them using the Expectation Maximization algorithm. Thus, whereas FastBIC is guaranteed to obtain the global maximum likelihood estimator, BIC is liable to find only a local maximum. The algorithm to estimate μ_k, π_k and z_k is provided in Algorithm 4.

3.4.3 Proximity Matrix Construction

The proximity matrix S for input data $D \in \mathbb{R}^{n \times d}$ is estimated using the unsupervised random forest by simply counting the fraction of times that a pair of points occurs in the same leaf node in the forest. Thus $S(i,j) = S_{ij} = \frac{L_{ij}}{T_{ij}}$, where $L(i,j)$ is the number of occurrences of points i and j in the same leaf node, and T_{ij} is the number of trees in which both point i and point j were included in the sample R that was used to build the tree.

3.5 Algorithms

Algorithm 1 Build a random forest using unlabeled data

procedure BUILDURF(X, T, d, c)
  for $i = 1, 2, \ldots, T$ **do**
    $S \leftarrow$ random sample (with replacement) from X of size m
    $t_i =$**BuildTree**$(S, d, c, 0)$
    $F \leftarrow F \cup \{t_i\}$
    return F
  end for
end procedure

Algorithm 2 Build an unsupervised decision tree

procedure BUILDTREE(Y, d, c, k, depth)
  if $|Y| \leq c$ OR depth == d **then**
    return LeafNode(Y, depth) ▷ Create a leaf node
  else
    $\mathcal{C} \leftarrow$ random sample of size k from $\{1, \ldots, d\}$
    min_dists $\leftarrow \infty$
    for $i \in$ C **do**
      $Y^{(i)} \leftarrow Y\,[, i]$
      (midpt, sum_sq_dists) = **OneD**$(Y^{(i)})$
      if (sum_sq_dists <min_dists) **then**
        best_dim = i
        best_split_pt = midpt
      end if
    end for
    $Y_{\text{left}} = \{y \in Y | y(\text{best\_dim}) < \text{best\_split\_pt}\}$
    $Y_{\text{right}} = \{y \in Y | y(\text{best\_dim}) \geq \text{best\_split\_pt}\}$
    new_Node = CreateInternalNode(best_split_pt, best_dim, depth)
    new_Node.leftChild = BuildTree(Y_{left}, d, c, k, depth+1)
    new_Node.rightChild = BuildTree(Y_{right}, d, c, k, depth+1)
    return new_Node
  end if
end procedure

Algorithm 3 Find the optimal split, in terms of the k-means objective, of one-dimensional data with k=2

procedure UNIVARIATETWOMEANS($Z = \{z | z \in \mathcal{R}^1\}$)
  $\mu_1 \leftarrow \min_{z \in Z} z$
  $\mathcal{C}_1 \leftarrow \{\mu_l\}$
  $\mathcal{C}_2 \leftarrow Z \backslash \mathcal{C}_1$
  $\mu_2 \leftarrow \frac{1}{|C_2|} \sum_{z_i \in C_2} z_i$ ▷ mean of C_2
  dists_sq $\leftarrow \sum_{j=1}^{2} \sum_{z_i \in \text{set}_j} (z_i - \mu_j)^2$
  min_dist_sq $\leftarrow$ dists_sq
  while set$_2 \neq \emptyset$ **do**
    $z \leftarrow \min(\text{set}_2)$
    $\mathcal{C}_1 \leftarrow \mathcal{C}_1 \cup \{z\}$
    $\mathcal{C}_2 \leftarrow \mathcal{C}_2 \setminus \{z\}$
    $\mu_1 \leftarrow \frac{1}{|C_1|} \sum_{z_i \in C_1} z_i$ ▷ mean of C_1
    $\mu_2 \leftarrow \frac{1}{|C_2|} \sum_{z_i \in C_2} z_i$ ▷ mean of C_2
    dists_sq $\leftarrow \sum_{j=1}^{2} \sum_{z_i \in \mathcal{C}_j} (z_i - \mu_j)^2$
    if dists_sq $<$ min_dist_sq **then**
      min_dists_sq $\leftarrow$ dists_sq
      best_midpt $\leftarrow (\max(\mathcal{C}_1) + \min(\mathcal{C}_2))/2$ ▷ Midpoint between C_1 and C_2
    end if
  end while
  return (best_midpt, min_dist_sq)
end procedure

Algorithm 4 Find the optimal split, in terms of BIC score, of one-dimensional data with k=2 assumming the GMM Model

procedure GMM(Initialized estimates)
  $z_{n,k} = \frac{\mathcal{N}(x_n|\mu_k,\sigma^2)\pi_k}{\sum_{k'} \mathcal{N}(x_n|\mu_{k'},\sigma^2)\pi_{k'}}$
  $\pi_k = \frac{1}{N} \sum_n z_{n,k}$
  $\mu_k = \sum_n \frac{z_{n,k}}{\sum_{n'} z_{n',k}}$
  $\sigma^2 = \frac{1}{N} \sum_n \sum_k z_{n,k} ||x_n - \mu_k||^2$
end procedure

Algorithm 5 Find the optimal split, in terms of BIC score, of one-dimensional data with k=2

procedure ONED($Z = \{z | z \in \mathcal{R}^1\}$)
  $\mu_1 \leftarrow \min_{z \in Z} z$
  $\mathcal{C}_1 \leftarrow \{\mu_l\}$
  $\mathcal{C}_2 \leftarrow Z \setminus \mathcal{C}_1$
  $\mu_2 \leftarrow \frac{1}{|C_2|} \sum_{z_i \in C_2} z_i$ ▷ mean of C_2
  BIC_curr $\leftarrow \sum_{j=1}^{2} \sum_{z_i \in \text{set}_j} (z_i - \mu_j)^2$
  min_BIC_curr $\leftarrow$ dists_sq
  while $\text{set}_2 \neq \emptyset$ **do**
    $z \leftarrow \min(\text{set}_2)$
    $\mathcal{C}_1 \leftarrow \mathcal{C}_1 \cup \{z\}$
    $\mathcal{C}_2 \leftarrow \mathcal{C}_2 \setminus \{z\}$
    $\mu_1 \leftarrow \frac{1}{|C_1|} \sum_{z_i \in C_1} z_i$ ▷ mean of C_1
    $\mu_2 \leftarrow \frac{1}{|C_2|} \sum_{z_i \in C_2} z_i$ ▷ mean of C_2
    $\sigma_1^2 \leftarrow \frac{1}{|C_1|}(z_1 - \mu_1)^2$
    $\sigma_2^2 \leftarrow \frac{1}{|C_2|}(z_2 - \mu_2)^2$
    $\sigma_{\text{comb}}^2 \leftarrow \frac{1}{|C_1|+|C_2|} \sum_{j=1}^{2} \sum_{z_i \in \mathcal{C}_j} (z_i - \mu_j)^2$
    BIC_diff_var $\leftarrow -2(|C_1| \log \frac{|C_1|}{|C_1|+|C_2|} - \frac{|C_1|}{2} \log 2\pi\sigma_1^2 - |C_2| \log \frac{|C_1|}{|C_1|+|C_2|} + \frac{|C_2|}{2} \log 2\pi\sigma_2^2) + \ln(3)(|C_1| + |C_2|)$
    BIC_same_var $\leftarrow -2(|C_1| \log \frac{|C_1|}{|C_1|+|C_2|} - \frac{|C_1|}{2} \log 2\pi\sigma_{\text{comb}}^2 - |C_2| \log \frac{|C_1|}{|C_1|+|C_2|} + \frac{|C_2|}{2} \log 2\pi\sigma_{\text{comb}}^2) + \ln(2)(|C_1| + |C_2|)$
    BIC_curr $\leftarrow$ min ((BIC_same_var, BIC_diff_var)
    if BIC_curr $<$ min_BIC **then**
      min_BIC $\leftarrow$ BIC_curr
      best_midpt $\leftarrow (\max(\mathcal{C}_1) + \min(\mathcal{C}_2))/2$ ▷ Midpoint between C_1 and C_2
    end if
  end while
  return (best_midpt, min_BIC)
end procedure

Bibliography

A. Y. Alfakih, A. Khandani, and H. Wolkowicz. Solving Euclidean distance matrix completion problems via semidefinite programming. *Computational Optimization and Applications*, 12(1):13–30, Jan 1999. ISSN 1573-2894. doi: 10.1023/A:1008655427845. URL https://doi.org/10.1023/A:1008655427845.

A. Athreya, C. E. Priebe, M. Tang, V. Lyzinski, D. J. Marchette, and D. L. Sussman. A limit theorem for scaled eigenvectors of random dot product graphs. *Sankhya A*, 78(1):1–18, Feb 2016. ISSN 0976-8378. doi: 10.1007/s13171-015-0071-x. URL https://doi.org/10.1007/s13171-015-0071-x.

M. Bakonyi and C. Johnson. The Euclidian distance matrix completion problem. *SIAM Journal on Matrix Analysis and Applications*, 16(2):646–654, 1995. doi: 10.1137/S0895479893249757. URL https://doi.org/10.1137/S0895479893249757.

Mikhail Belkin and Partha Niyogi. Laplacian eigenmaps and spectral techniques for embedding and clustering. In *Advances in neural information processing systems*, pages 585–591, 2002.

BIBLIOGRAPHY

I. Borg and P. J. F. Groenen. *Modern Multidimensional Scaling: Theory and Applications*. Springer, New York, 2005.

Leo Breiman. Random forests. *Machine learning*, 45(1):5–32, 2001.

J. D. Carroll and J.-J. Chang. Analysis of individual differences in multidimensional scaling via an n-way generalization of "Eckart-Young" decomposition. *Psychometrika*, 35(3):283–319, Sep. 1970. ISSN 1860-0980. doi: 10.1007/BF02310791. URL https://doi.org/10.1007/BF02310791.

S. Chatterjee. Matrix estimation by universal singular value thresholding. *The Annals of Statistics*, 43(1):177–214, 2015. doi: 10.1214/14-AOS1272.

L. Chen and A. Buja. Local multidimensional scaling for nonlinear dimension reduction, graph drawing, and proximity analysis. *Journal of the American Statistical Association*, 104(485):209–219, 2009. doi: 10.1198/jasa.2009.0111. URL https://doi.org/10.1198/jasa.2009.0111.

M. A. A. Cox and T. F. Cox. *Multidimensional Scaling*, pages 315–347. Springer Berlin Heidelberg, Berlin, Heidelberg, 2008. ISBN 978-3-540-33037-0. doi: 10.1007/978-3-540-33037-0_14. URL https://doi.org/10.1007/978-3-540-33037-0_14.

Trevor F Cox and Michael AA Cox. *Multidimensional scaling*. Chapman and hall/CRC, 2000.

A. Criminisi and J. Shotton. Manifold forests. In A. Criminisi and J. Shotton, editors,

Decision Forests for Computer Vision and Medical Image Analysis, chapter 7, pages 79–94. Springer, London, 2013.

C. Davis and M. Kahan, W. The rotation of eigenvectors by a perturbation III. *SIAM Journal of Numerical Analysis*, 7:1–46, 1970.

J. de Leeuw and W. Heiser. Theory of multidimensional scaling. In P.R. Krishnaiah and L. Kanal, editors, *Handbook of Statistics II*, pages 285–316. North Holland Publishing Company, Amsterdam, The Netherlands, 1982.

Luc Devroye, Laszlo Györfi, and Gabor Lugosi. *A Probabilistic Theory of Pattern Recognition (Stochastic Modelling and Applied Probability)*. Springer, corrected edition edition, February 1997.

J. Fan, Q. Sun, W. X. Zhou, and Z. Zhu. Principal component analysis for big data, January 2018. arXiv:1801.01602.

J. Glaunès, A. Qiu, M. I. Miller, and L. Younes. Large deformation diffeomorphic metric curve mapping. *International Journal of Computer Vision*, 80(3):317–336, 2008. ISSN 0920-5691. URL `http://dx.doi.org/10.1007/s11263-008-0141-9`.

Harold Hotelling. Relations between two sets of variates. *Biometrika*, 28(3/4):321–377, 1936.

Aapo Hyvärinen and Erkki Oja. Independent component analysis: algorithms and applications. *Neural networks*, 13(4-5):411–430, 2000.

BIBLIOGRAPHY

J. E. Jackson. *A User's Guide to Principal Components*. Wiley & Sons, New York, 1991.

A. Javanmard and A. Montanari. Localization from incomplete noisy distance measurements. *Foundations of Computational Mathematics*, 13(3):297–345, Jun 2013. ISSN 1615-3383. doi: 10.1007/s10208-012-9129-5. URL https://doi.org/10.1007/s10208-012-9129-5.

I. Kaltenmark, B. Charlier, and N. Charon. A general framework for curve and surface comparison and registration with oriented varifolds. *Computer Vision and Pattern Recognition (CVPR)*, 2017.

K. Levin, A. Athreya, M. Tang, V. Lyzinski, and C. E. Priebe. A central limit theorem for an omnibus embedding of random dot product graphs, 05 2017. arXiv:1705.09355.

Andy Liaw and Matthew Wiener. Classification and regression by randomforest. *R News*, 2(3):18–22, 2002.

Laurens van der Maaten and Geoffrey Hinton. Visualizing data using t-sne. *Journal of machine learning research*, 9(Nov):2579–2605, 2008.

J. A. T. Machado and M. E. Mata. Analysis of world economic variables using multidimensional scaling. *PLOS ONE*, 10(3):1–17, 03 2015. doi: 10.1371/journal.pone.0121277. URL https://doi.org/10.1371/journal.pone.0121277.

BIBLIOGRAPHY

Michael W Mahoney and Petros Drineas. Cur matrix decompositions for improved data analysis. *Proceedings of the National Academy of Sciences*, pages pnas–0803205106, 2009.

Leland McInnes and John Healy. Umap: Uniform manifold approximation and projection for dimension reduction. *arXiv preprint arXiv:1802.03426*, 2018.

Marius Muja and David G Lowe. Scalable nearest neighbor algorithms for high dimensional data. *IEEE Transactions on Pattern Analysis & Machine Intelligence*, 36(11):2227–2240, 2014.

S. Oh, A. Montanari, and A. Karbasi. Sensor network localization from local connectivity: Performance analysis for the mds-map algorithm. In *2010 IEEE Information Theory Workshop on Information Theory (ITW 2010, Cairo)*, pages 1–5, Jan 2010. doi: 10.1109/ITWKSPS.2010.5503144.

N. Patwari, J. N. Ash, S. Kyperountas, A. O. Hero, R. L. Moses, and N. S. Correal. Locating the nodes: cooperative localization in wireless sensor networks. *IEEE Signal Processing Magazine*, 22(4):54–69, July 2005. ISSN 1053-5888. doi: 10.1109/MSP.2005.1458287.

Karl Pearson. Liii. on lines and planes of closest fit to systems of points in space. *The London, Edinburgh, and Dublin Philosophical Magazine and Journal of Science*, 2 (11):559–572, 1901.

BIBLIOGRAPHY

E. Pekalska and R. P. W. Duin. *The Dissimilarity Representation for Pattern Recognition: Foundations and Applications*. World Scientific Publishing Company Inc, Singapore, 2005.

E. Peterfreund and M. Gavish. Multidimensional Scaling of Noisy High Dimensional Data, January 2018. arXiv:1801.10229.

B. Schölkopf, A. Smola, and K.-R. Müller. Nonlinear component analysis as a kernel eigenvalue problem. *Neural Computation*, 10(5):1299–1319, 1998. doi: 10.1162/089976698300017467. URL `https://doi.org/10.1162/089976698300017467`.

Bernhard Schölkopf, Alexander Smola, and Klaus-Robert Müller. Kernel principal component analysis. In *International Conference on Artificial Neural Networks*, pages 583–588. Springer, 1997.

Tao Shi and Steve Horvath. Unsupervised learning with random forest predictors. *J. Comput. Graph. Stat.*, 15(1):118–138, March 2006.

A. Singer. A remark on global positioning from local distances. *Proceedings of the National Academy of Sciences*, 105(28):9507–9511, 2008. ISSN 0027-8424. doi: 10.1073/pnas.0709842104. URL `http://www.pnas.org/content/105/28/9507`.

I. Spence and D. W. Domoney. Single subject incomplete designs for nonmetric multidimensional scaling. *Psychometrika*, 39(4):469–490, Dec 1974. ISSN 1860-0980. doi: 10.1007/BF02291669. URL `https://doi.org/10.1007/BF02291669`.

BIBLIOGRAPHY

Mohammad J. Taghizadeh. Theoretical analysis of euclidean distance matrix completion for ad hoc microphone array calibration. Idiap-RR Idiap-RR-20-2014, Idiap, 11 2014.

A. Tasissa and R. Lai. Exact reconstruction of Euclidean distance geometry problem using low-rank matrix completion. *CoRR*, abs/1804.04310, 2018.

J. B. Tenenbaum, V. D. Silva, and J. C. Langford. A global geometric framework for nonlinear dimensionality reduction. *Science*, 290(5500):2319–2323, 2000a. ISSN 0036-8075. doi: 10.1126/science.290.5500.2319. URL `http://science.sciencemag.org/content/290/5500/2319`.

Joshua B Tenenbaum, Vin De Silva, and John C Langford. A global geometric framework for nonlinear dimensionality reduction. *science*, 290(5500):2319–2323, 2000b.

Tyler M Tomita, Mauro Maggioni, and Joshua T Vogelstein. Randomer forests. *arXiv preprint arXiv:1506.03410*, 2015.

W. S. Torgerson. Multidimensional scaling: I. theory and method. *Psychometrika*, 17:401–419, 1952.

Roman Vershynin. *High-Dimensional Probability: An Introduction with Applications in Data Science*. Cambridge Series in Statistical and Probabilistic Mathematics. Cambridge University Press, 2018. doi: 10.1017/9781108231596.

BIBLIOGRAPHY

J. T. Vogelstein, Y. Park, T. Ohyama, R. A. Kerr, J. W. Truman, C. E. Priebe, and M. Zlatic. Discovery of brainwide neural-behavioral maps via multiscale unsupervised structure learning. *Science*, 344(6182):386–392, 2014. ISSN 0036-8075. doi: 10.1126/science.1250298. URL `http://science.sciencemag.org/content/344/6182/386`.

Kilian Q Weinberger and Lawrence K Saul. Unsupervised learning of image manifolds by semidefinite programming. *International journal of computer vision*, 70(1):77–90, 2006.

Y. Yu, T. Wang, and R. J. Samworth. A useful variant of the Davis-Kahan theorem for statisticians. *Biometrika*, 102:351–323, 2015.

L. Zhang, G. Wahba, and M. Yuan. Distance shrinkage and Euclidean embedding via regularized kernel estimation. *Journal of the Royal Statistical Society: Series B (Statistical Methodology)*, 78(4):849–867, 2016. doi: 10.1111/rssb.12138. URL `https://rss.onlinelibrary.wiley.com/doi/abs/10.1111/rssb.12138`.

M. Zhu and A. Ghodsi. Automatic dimensionality selection from the scree plot via the use of profile likelihood. *Computational Statistics and Data Analysis*, 51(2):918 – 930, 2006.

Vita

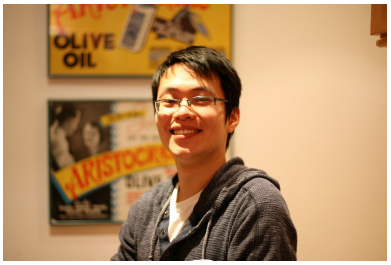

Gongkai (Percy) Li received the B.S. degree in mathematics from the Lehigh University in 2014, the M.S.E. degree in Applied Mathematics and Statistics from the Johns Hopkins University in 2017 and enrolled in the Applied Mathematics and Statistics Ph.D. program at Johns Hopkins University in 2014. He has received the Teaching Fellow Recognition Award.